

POWER SYSTEM FOR A HUMANOID

Nathaniel Brewer

Submitted for the degree of
Bachelor of Engineering (Honours) in the division of
Electrical Engineering
October 2001.

Department of Information Technology and Electrical Engineering
University of Queensland

104 Cedar St
Wynnum QLD 4178
19th October 2001

The Head
School of Information Technology and Electrical Engineering
University of Queensland
St Lucia QLD 4072

Dear Professor Kaplan

In partial fulfilment of the requirements of the degree of Bachelor of Engineering (Honours) in the division of Electrical Engineering, I present this Thesis entitled "Power Systems for a Humanoid". This thesis was conducted under the supervision of Dr Gordon Wyeth and as part of the GuRoo Project.

I declare that the work presented herein is my own and has not previously been submitted for any other form of assessment. Care has been taken to reference all work conducted by other persons or entities and to the best of my knowledge has been referenced in the text.

Yours sincerely

Nathaniel Brewer

Acknowledgements

I must thank Gordon for providing an interesting but difficult topic, whose requirements changed and changed, and... also for the ability to buy components that he knew not where nor why they went.. I thank Geoff for telling me what I was actually doing, so the subjects in second semester, dope.

I must also thank the GuRoo team and the rest of the lab.

Bartek, for making PCB design interesting, and for trying to keep me on track. Tim, for occasionally being in the Lab. Jared for never being there the same time as Tim Shane, for dialogue of confused tired lab, guys. Damien for not caring about power, give me torque. Mark, for not caring about anyone. Andrew, for insight into the world around us. David for his sly interpretation of things. Emanuel for making control so simple. Andrew (Shmittty) for never leaving the labs, and making the world seem such a twisted place. Mark Venz, so what is a pointer again? Ilan, for a thesis that actually seemed to work. Sarah, for keeping the lab slightly sane. Jun and Rex for doing their best to stop this.

Abstract

This thesis describes the steps taken to evaluate design and construct a power supply for a mobile humanoid. The power supply must be able to handle the varied loads of the humanoid, which consist of a high average power but also the very high peak power requirements. The GuRoo team at the University of Queensland is aiming to produce a humanoid that is capable of playing soccer. This GuRoo project will continue for a number of years at UQ, with each year's students progressing further along with the evolution of the humanoid. The aim for this year was to assemble the systems necessary for the GuRoo to be able to walk.

This thesis presents the design of the power system of the humanoid. One of the difficult tasks was to estimate the power consumption of the humanoid before it was built. It was found that estimates are very perspective and capable of reaching extremes. Even with the help of a full mechanical simulator, it was difficult to get accurate estimates as the rapid change in the mechanical design and walking algorithm led to a corresponding rapid change in the power consumption. A final estimate of 800W for the lower body joints seemed to gain approval from both the mechanical design team and the control systems team. This figure was used in the design of the power system.

A number of Ni-Cd battery packs were made available second hand from the Sunshark team. These consisted of 32, 1.5Ah Ni-Cd cells which in total deliver between 35 to 44V and can source up to 6A for each pack. The desired voltage for the motor drivers was above 32V and to provide the 800W for 20 minutes it was necessary to place four of these packs in parallel. In order to allow the packs to be placed in parallel and to ensure even current sharing, this thesis details a parallel scheme that uses buck converters on each battery pack to control both the output voltage of the system and the current sharing between the packs. The final product is able to deliver over 1kW of power and from latest estimates should be able to power the GuRoo for over 20mins, or one half of the Robo Cup Humanoid soccer league game.

Table of Contents

CHAPTER 1	INTRODUCTION.....	1
1.1	THESIS MOTIVATION.....	1
1.2	THE GUROO.....	1
1.3	POWER SYSTEMS IN THE HUMANOID.....	2
1.4	CHAPTER OUTLINE.....	4
CHAPTER 2	LITERATURE REVIEW.....	6
2.1	POWER SOURCES.....	6
2.1.1	<i>Batteries</i>	7
2.1.2	<i>Humanoids</i>	8
2.2	BUCK CONVERTERS.....	8
2.2.1	<i>Applications</i>	8
2.2.2	<i>Operation</i>	9
2.2.3	<i>Theory</i>	10
2.2.4	<i>Control</i>	11
2.3	PARALLEL SUPPLIES.....	12
2.3.1	<i>Problems</i>	13
2.3.2	<i>Solutions</i>	14
2.3.3	<i>Buck converters in current sharing</i>	16
CHAPTER 3	EVALUATING POWER CONSUMPTION.....	18
3.1	INITIAL ESTIMATES.....	18
3.2	SIMULATOR RESULTS.....	20
3.3	DESIGN REQUIREMENTS.....	24
CHAPTER 4	POWER SOURCES.....	26
4.1	BATTERY SELECTION.....	26
4.2	CHARGING REQUIREMENTS.....	30

4.3	DISCHARGE CHARACTERISTICS	31
4.4	BATTERY PCB AND CONNECTION	32
CHAPTER 5 POWER SUPPLY HARDWARE.....		33
5.1	POWER SUPPLY CONFIGURATION.....	34
5.2	BUCK CONVERTER DESIGN	36
5.3	HARDWARE DESIGN.....	37
5.3.1	<i>Buck converter</i>	38
5.3.1.1	MOSFETs	38
5.3.1.2	MOSFET Drivers.....	39
5.3.1.3	Signal Buffers	41
5.3.1.4	Diodes	41
5.3.1.5	Inductors.....	42
5.3.1.6	Capacitors.....	42
5.3.1.7	Current Sensors	43
5.3.2	<i>Measurements</i>	44
5.3.2.1	Temperature sensors	44
5.3.2.2	Voltage measurement.....	44
5.3.2.3	Multiplexers	45
5.3.2.4	Buffer Amplifiers.....	45
5.3.3	<i>Power regulators</i>	46
5.3.3.1	5V Regulator	46
5.3.3.2	12 Boost Regulator.....	46
5.3.4	<i>Servo Supply</i>	47
5.3.5	<i>TMS320F243</i>	48
5.4	PCB LAYOUT	49
5.5	CONSTRUCTION AND TESTING	50
5.6	WIRING HARNESS	52
5.7	MOUNTING THE POWER SYSTEM.....	53

CHAPTER 6	CONTROL OF THE POWER SUPPLY.....	54
6.1	REQUIREMENTS OF CONTROL	54
6.2	POWER PROPORTIONING ALGORITHM	56
6.3	BUCK CONVERTER CONTROL	57
6.4	AVOIDING INSTABILITY	60
CHAPTER 7	RESULTS.....	61
CHAPTER 8	CONCLUSION.....	63
BIBLIOGRAPHY	65
APPENDIX	70

Table of figures

Figure 2-1	Buck Converter with variable load.....	9
Figure 2-2	Parallel sources with revers bias protection	15
Figure 3-1	Early Simulation of Power Requirements.....	21
Figure 3-2	Simulation of Power Requirements as of 10/10/2001.....	22
Figure 4-1	42V NiCd Battery Packs (3 of)	30
Figure 5-3	Buck Converter Schematic.....	38
Figure 5-4	MOSFET Driver.....	40
Figure 5-5	Current Sensor.....	43
Figure 5-6	12V Boost Converter.....	47
Figure 5-7	GuRoo Mounting of Power System [50].....	53
Figure 6-1	Control Diagram.....	56
Figure 6-2	Control diagram for Buck Converters.....	59
Figure 0-1	Power Output vs. Source Current Batteries with diodes in series, all sources at 35V, 3 at 1 Ω , 1 at 0.9 Ω	70
Figure 0-2	Power out (kW) vs. Source Current (A). All sources at 1 Ω , 3 at 35V one at 35.5V	71

Figure 0-3 Power out (kW) vs Source Current (A), ideal case all at 35V 1Ω.....	72
Figure 0-4 Power Board PCB	73

Chapter 1 Introduction

1.1 Thesis Motivation

The purpose of this thesis is to design and construct a power system for use in the humanoid robot, being developed at the University of Queensland (UQ). The humanoid is affectionately known as the GuRoo, or Grossly Under funded Roo, (the suffix Roo is a tradition at UQ). This is due to the significantly lower budget for the humanoid project than that of rival projects such as at Honda and Sony.

The overall goal of the humanoid project is to make a humanoid that is capable of playing soccer against other humanoid robots at the world Robocup competition. RoboCup is an annual competition whose aim is to promote research and engineering effort into robotics, in part by the use of the game of soccer. One objective of RoboCup is to produce a team of humanoids that could beat the World Cup soccer team, by the year 2050 [44].

In order to play soccer effectively, a humanoid needs to be free of any tether as any external cables are bound to trip up one robot or another. Therefore, it is essentially that the power system and power sources are all on board the robot. This adds the challenge of not only having to meet power requirements but also those of running time, weight, size and durability.

1.2 The GuRoo

In order for a humanoid to effectively play soccer, not only must it be able to stand and walk, but it must also be able to see a ball, think about kicking it and manoeuvre itself into a position where a kick could score a goal. Inside the humanoid, there are a

number of systems needed to meet these objectives. A brain in the form of an IPAQ, eyes in the form of a CMOS camera [3], an optical nerve consisting of an SH4 processor and a parallel IPAQ connector [11]. A spinal cord and nervous system consisting of a USB port from the IPAQ connected through a gateway to a CAN network [1]. Muscles [18] in the lower body consist of 15 Maxon RE36 motors and Joint controller boards [5] and upper body muscles consist of eight servomotors and a servo controller board [48]. The power system must supply power to these 10 electronics board, IPAQ, 8 servomotors and 15 high power motors.

The humanoid will stand at approximately 1.2 meters tall and will have a mass of around 40kg [50][18]. This is already quite heavy for a person of this size [52] and it is therefore necessary to keep the weight of the power supply as low as possible, even if this means sacrificing running time. The power supply and batteries will be situated in the chest of the humanoid. They will thus also have to meet considerable size restrictions for such a high power system.

The power sources for the humanoid consist of four 42V 1.5Ah NiCd batteries plus an additional two, 7.2V 3Ah NiCd batteries. The two 7.2V batteries are used separately to supply power to the electronics boards and the servomotors. This isolates the electronics boards from faults on the servos and allows a longer run time for the digital boards, useful in testing.

1.3 Power Systems in the Humanoid

The humanoid has three different types of load; [1] 15 high power motors, 8 low power Hi-Tech RC servos 6V at a maximum 0.75A each and 10 electronics boards at 7.2V. Of the electronic boards five are high power joint controller boards, each controlling three motors. These joint controller boards and associated motors demand the most from the power system. These boards are placed near their respective motors in the lower leg, upper leg and hip.

Due to this configuration, it is quite common for one board to draw high power for all motors simultaneously. The power load for one board will therefore vary from high loads to rather light loads depending on the stage of a step cycle. The use of a common bus allows the heavy load of one board to be offset by the lighter loads of another. This results in a reduction of the ratio of the peak to average currents and will result in the need for a less rugged power supply. During one full step cycle, the high power motors in the humanoid draw an average of 66W current while peaks associated with motor start-ups and high loading can be as high as 175W. The power drawn is very uneven and peak currents can last from 250ms to over 1s.

Certain battery packs were made available second hand from the Sunshark team. Due to the restricted budget of the humanoid project and the low cost of these batteries, it was necessary to find a way to utilize them for this project. The batteries consisted of 32, 1.5Ah P-150AS, nickel cadmium cells in series giving a voltage of around 42V and a loaded voltage of around 38V. As one pack could not singly provide enough power, it became necessary to parallel the packs to arrive at a sufficient current.

When placing battery packs in parallel, a number of possible problems can occur. These include current recirculation, uneven internal impedances leading to different discharge rates and the possibility of badly charged or non-charged batteries wrongly being connected with fully charged ones. These problems can, not only lead to a reduction of the performance of the power supply, but can also be potentially dangerous.

Due to these problems, there is a need for a method to protect the batteries and ensure an even load distribution. The solution presented here involves regulating the current from each battery using a buck converter. The output of these converters is connected to a common bus, which is then run to each of the five high power control boards. This allows the current load to be actively shared in an intelligent manner. It allows lower

voltage or higher temperature batteries to take less of the load thus reducing the strain on them and improving the efficiency, and run time of the high power system.

The Buck converters are controlled by a TMS320F241 from Texas Instruments. This chip also monitors all battery voltages and temperatures, and the current from the 42V batteries. The electronics for the power supply are mounted on a single PCB, which also contains an interface between a USB port and the CAN network throughout the humanoid, implemented using the same microprocessor. The Power supply is able to source 600W continuously with peaks up to 40A on the 42V bus and 6A continuously on both 7.2V buses. The supply is expected to be able to run the humanoid for over 20 minutes.

1.4 Chapter Outline

In chapter two the thesis will discuss previous approaches to mobile power supplies and supplies for robotics. In addition, literature discussing, battery selection, the design of Buck converters, the use and types of Parallel supplies and current sharing control schemes will be reviewed.

Chapter 3 will discuss how the estimates for the power requirements of the humanoid were obtained. It will examine how the results from the simulator affected the design requirements. This chapter will define what the desired operating parameters of the power supply will be.

Chapter 4 will go into detail about the selection of a power source. It will discuss the charge and discharge characteristics of the selected batteries, including internal impedance, current and temperature limitations. The charging of Ni-Cd batteries and the battery PCB will be examined.

Chapter 5 will discuss the design of the power supply board. This will include the design and implementation of buck converters, temperature and current sensors, and the digital controller. Component selection and PCB design where both time consuming tasks and will be presented in some detail.

Chapter 6 will present the methods used for controlling the power supply. This will include the control loops for the Buck converters and the current sharing algorithm. It will examine the requirements of monitoring the charge and condition of batteries and protecting their health by current limiting.

Chapter 7 will examine the performance of the system in its current state of completion.

Chapter 8 will examine the success and failures of this thesis project. It will look at work yet to be completed and the future directions for the project.

Chapter 2 Literature review

2.1 Power sources

There were a number of possible power sources considered for use in the humanoid. These include; fuel cells, internal combustion engines coupled with generators, mechanical storage elements, such as flywheels, and batteries. A number of selection criteria must be applied when selecting between these sources. The most apparent are those of available power and energy, combined with the weight to achieve these. Other factors are the reliability, safety, cost, ease of recharge or replenishment, and the impact it will have on the design and construction of the humanoid.

In the future fuel cells offer the promise of providing cheap energy storage. They use fuels such as Hydrogen or Methane and use an oxidation process across a membrane to produce electricity. Usually the only by-product is water and carbon dioxide when methane is used. Currently fuel cells have not been scaled to the appropriate sizes that would make them practical for use in a humanoid. They have not reached the power to weight or power to volume levels that are required. Fuel cells offer the ability to be refuelled quickly. They also, operate quietly and produce low emissions, making them suitable for indoor use. As the technology improves, they may become more appealing.

Internal Combustion engines running off petrol or natural gas, offer very high energy to weight and volume levels [6]. When they are combined with high frequency alternators, power to mass ratios in the order of 1kW/kg are obtainable. They are easily refuelled with readily available fuels. The biggest drawbacks to the use of combustion engines in the humanoid are that of exhaust and noise. As the humanoid will be used indoors, there is no guarantee that adequate ventilation will be provide. There would also not be much appreciation for the noise of a two stroke motor running at up to 500rps.

Mechanical Storage elements such as generator-flywheels are old technologies used in new applications. To store energy a flywheel is accelerated to very high rates of revolution. The kinetic energy of the flywheel can be converted into electricity using a generator or alternator. In order to counterbalance the inertia caused by a flywheel, two contra rotating wheels must be placed on the same axis [6]. Unfortunately, the overall systems are still too large to be practical for a humanoid although their size is being reduced.

2.1.1 Batteries

The most obvious and in the end most practical choice is to use rechargeable batteries. They offer reasonably high power and energy densities, without the associated noise and exhaust produced by engines. They do not require extensive maintenance or skilled installation. Batteries offer the advantage of a direct production of electricity, which will power the motors and electronics. Sealed batteries are not affected by orientation, and can be mounted easily in enclosed spaces. In addition, batteries are rugged and can survive reasonable intensity shocks, which may be encountered during operation.

With the increasing number of portable electrical devices, the portable energy storage market has increased considerably. As a result, there are now a number of different battery types and chemistries that are commercially available in mainstream production. The older nickel cadmium (Ni-Cd) batteries, the higher energy density lithium ion (Li Ion), and the less toxic nickel metal hydride (NiMH).

The extensive range of cell types provides a vast range of power and energy densities. There are cells specifically designed for high discharge rates and for operating in harsh conditions. The options presented by batteries make them a good choice for use in the GuRoo.

2.1.2 Humanoids

There are very few examples of walking humanoids, let alone those with onboard power supplies. The most famous of these are the P2, P3 and ASIMO from Honda and the SDR-3X from Sony.

Honda's P3 humanoid weighs 130kg and is 1.6m tall [9]. It uses 138V 6Ah nickel Zinc (Ni-Zn) batteries giving 830Wh of energy and an estimated power output of above 3kW. Honda's ASIMO robot weighs 43kg and is 1.2m tall [10]. This is the closest in size and weight to that planned for the GuRoo. The ASIMO uses 38.4V 10Ah NiMH batteries (probably 32x1.2V cells) giving a stored energy of 384Wh and an estimated power of 1.1kW. This power supply arrangement closely resembles that described in Chapter 4.

Published data such as power requirements, run time and weight are very limited. Only commercial companies have progressed far enough into the design process to have this type of data, and they are not keen to share.

2.2 Buck Converters

2.2.1 Applications

Switch mode power supplies (SMPS) are increasingly managing to find their way into commercial products. This is due to their high efficiency and relatively small size and weight [24]. DC-DC switch mode converters are found in products such as computers power supplies, portable computers and smart battery management [19]. Switch mode converters are also found in high power applications such as motor drivers, inverters, power factor corrections units and in parallel supply systems [22].

2.2.2 Operation

The basic principles behind switch mode converters, and in particular, buck converters, are quite simple and a good discussion can be found in [24]. A buck, or step down converter, produces a voltage lower than that of the input voltage. As an approximation the output voltage is proportional to input voltage and the duty cycle of the switch. To adjust the output voltage the duty cycle of the switch is varied by a pulse width modulated signal.

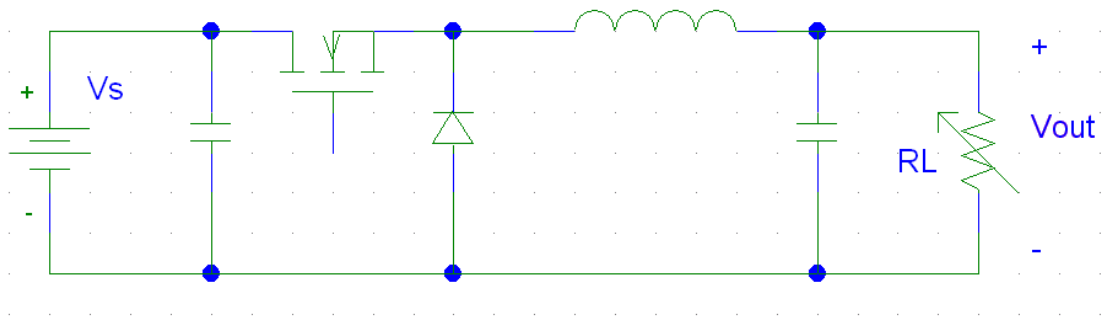


Figure 2-1 Buck Converter with variable load

When the switch is closed current flows from the power source through the switch and inductor into the capacitor and load. Energy is stored in the inductor as the current flows and the voltage on the capacitor increases. As current cannot change instantaneously in an inductor, when the switch is turned off a voltage develops across the inductor, which forward biases the diode, which then conducts current from ground. The energy stored in the inductor when the switch is closed, provides the energy for the current when the switch is open. In steady state, the current supplied during the off stage balances the extra energy stored in the inductor during the on stage.

Turning on and off the switch leads to a variation in the output current and voltage of the converter. In order to reduce these the values of the inductor and capacitor are made

as high as practical. Similarly increasing the frequency of the switching can result in smaller current and voltage variations or in a reduction in the size of the components. Current DC-DC converters operate from frequencies of 100kHz up to over 1MHz. These high frequencies allow the use of small components making the converters very practical [24].

2.2.3 Theory

While the basics of operation of buck converters is rather simple, the in depth analysis and modelling of converters can become quite complex. The nature of switches, such as MOSFETs, and the discontinuous nature of the process make it difficult to accurately model the full switch mode converter. Parasitic capacitances, inductances and the nonlinearly nature of diodes and MOSFETs, particularly at high frequencies, make this modelling complex.

A SMPS can operate in either continuous conduction mode (CCM) or discontinuous conduction mode (DCM). The difference is that in CCM, there is a continuous flow of current in the inductor where as in DCM, there is not. In DCM the output voltage is not a direct relationship to the duty cycle and depends on the load [24]. Due top this the control of a SMPS is easiest when it is operating in the linear CCM. In order to be operating in continuous conduction mode there is a minimum current that the load must draw. The equation below indicates the worst case, when the duty cycle is at 50%

$$I_{LB,max} = \frac{TsV_d}{8L} = \frac{10us \times 45V}{8 \times 100uH} = 0.5625A \quad [24]$$

For a specific duty cycle the minimum current can be found in terms of the $I_{LB,max}$.

$$I_L = 4I_{LB,max}(1-D)D \quad [24]$$

The output voltage ripple of a converter can be calculated for continuous conduction mode using the following equation. It is necessary to keep the output voltage ripple within reasonable bounds, as it will affect circuits that run off the output supply rail.

$$\Delta V_o = \frac{T_s V_o}{8 C L} (1 - D) T_s \quad [24]$$

Similarly the ripple current through the inductor and hence the output capacitor can be calculated. This is important in determining the required ripple current rating of the output capacitors.

$$\Delta I_L = \frac{V_o}{L} (1 - D) T_s \quad [24]$$

2.2.4 Control

The majority of converters are controlled using analogue controllers, which are configurable for many applications. Converters are usually controlled using one of two methods; the first is direct duty ratio control, or its modified form of feed forward voltage, and the second is current mode control.

In direct duty ratio control, the output voltage is compared with the desired voltage to produce an error voltage. For fixed frequency operation, the switch is turned on at the start of each period. This voltage is amplified and compared with a sawtooth waveform, with a frequency equal to the desired operating frequency. When the amplified error is equal to the sawtooth voltage the switch is turned off [6724].

In Current Mode Control (CMC), a second internal control loop controls either the inductor or switch current [24][21]. The outside control loop is still dependant on the difference between the output and required voltages. The difference is that the sawtooth waveform is now provided by the ramping of the current. The error voltage now determines the current provided to the output stage. Raising the average current will raise the output voltage. This direct control of the average current can allow CMC converters to be used in parallel. By setting the same error voltage to each converter, the currents should be the same, for similar circuits.

To investigate control schemes for converters the circuit models or simulations must be very detailed. Details such as parasitic capacitance and inductances in components and in wiring must be included. This makes modelling very difficult and fine-tuning of control loops have to be made for a final product. To alleviate some of these problems there is an increasing interest in controlling converters digitally [22]. This can be done using DSP chips or Application Specific Integrated Circuits (ASICs). These controllers usually run a PID control loop, but can include functions that are more advanced.

The great advantage of digital control is that the control scheme can be changed in software. The PID values can be tested and adjusted quickly to match a product, and its load and line conditions. There is also the possibility including easily adjustable control algorithms, to limit current, provide soft starting, and protect from overvoltage and undervoltage conditions. Digital controllers are also less affected by temperature fluctuations and ageing of components [24].

2.3 Parallel supplies

Power sources are placed in parallel to provide either a greater output power or a higher energy source. It has the advantage over series supplies in that components only have to handle a proportion of the total power. Parallel supplies can also provide some forms of redundancy for failed units. They also enable power sources to be added and

removed on the fly. If some form of load sharing is used, it is possible to place different types of sources in parallel to improve the characteristics of a power system. [51]

2.3.1 Problems

Without active current sharing, there will always be one source that will try to push out more current, than the others do. This will result in that source reaching its current limit first and limiting the power to that delivered at this level. Even slight differences in voltages, caused by different working lives can be problematic. In addition, different source impedances, which can be composed of cabling, connectors, switches, battery construction limits and PCB layout, can significantly affect the current ratios.

Once a source reaches the limit of its fuse, it will blow, and the remaining sources will have to carry the load. This increase in load can then send the next source to peak and blow. This process eventually leads to all of the batteries blowing their fuses, one after the other. A short peak loading on the power supply could lead to a chain reaction, which would stop the humanoid in its tracks.

In general, a linear battery powered supply, such as batteries in series, or connected straight in parallel, are only as strong as their weakest battery, and in some case, the strongest battery. The worst affects can happen when freshly charged batteries are used alongside batteries charged some time ago or semi discharged packs. The power supply must protect all of the sources and must start to shutdown if one is overstressed. Once one battery reaches its current limit, the supply must shut down or limit the load on that source. If it is not possible to limit the loading then the source must be shutdown. This will inturn place an additional load on the other sources, which may lead to them, shutting down.

For a battery based power supply a number of situations may arise that can cause problems. If packs are charged differently, there will be differences in voltage. Packs

that may be slightly damaged or stressed in the past may have a higher resistance. If a flat pack was accidentally placed in parallel with freshly charged packs, there could be large recirculation currents.

Many of these problems could be prevented by taking proper care when installing and charging batteries. They could also be prevented from causing damage if the power supply could refuse to start. However, this may not be practical in a competition environment, where there may not be time to change packs before or during a game of soccer. We would like a supply that would try to run as long as possible before shutting down

2.3.2 Solutions

Straight parallel connections offer no protection from reverse biasing. It would lead to minimal power consumption under ideal conditions if all the sources had the same properties. If it is possible that properties are significantly different, then it is necessary to include some reverse bias protection for the sources. One solution is to connect the sources with diodes in series (see Figure 2-2). This would stop any reverse biasing of the sources.

If a lower voltage source, such as a flat battery pack, were connected, the diode would be reverse biased and would not conduct any current. However, if the sources are all at the same voltage, problems can still occur. If there is a lower resistance in one source and diode combination, or a higher output voltage, there will be problems with current sharing. This imbalance may arise from a better constructed battery or battery connection circuits, it could also result from a diode that may have a lower forward voltage drop than others. It does not take a large impedance difference to cause a problem. In the appendix are some examples of simulations using a diode with a 0.5V

voltage drop and different source impedances and when there is a higher voltage battery.

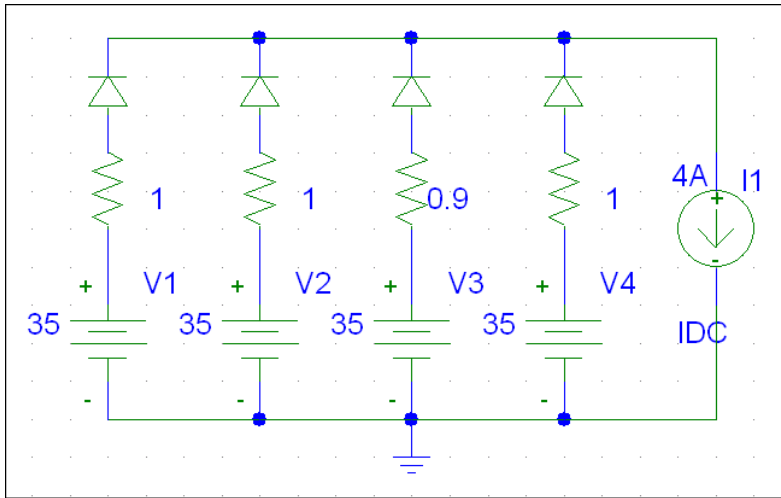


Figure 2-2 Parallel sources with revers bias protection

As can be seen, from graphs in the appendix a change in resistance of just 0.1Ω or a voltage difference of 1V can lead to one battery sourcing more current than the other. The power supply will always be limited by the battery sourcing the most current. In the above examples, this corresponds with a maximum power output loss of over 50W. In addition, there is also a fair amount of power being dissipated by the diodes. This power loss is no more than what would be present from an active current balancing scheme.

The diodes dissipate power proportional to the current and their forward voltage drop. Though still if there is difference in pack voltages, this will lead to a reduction in the maximum possible output power.

In general, for a linear system, if there is unevenness in either the source impedance or voltage, the maximum output power will be reduced from when they are perfectly

matched. This occurs even if there is one battery with a higher voltage or lower impedance than the rest.

To alleviate these problems an active form of current sharing should be used. This should be able to share the current between each pack to allow the maximum output power from the system while placing the least stress on the sources. In addition, an active sharing scheme could place a greater load on healthier sources, while trying to preserve others.

2.3.3 Buck converters in current sharing

To overcome these problems active current sharing can be accomplished by placing buck converters on the output of each source. By varying the duty cycle of the switches, the buck converters are effectively used as current converters instead of voltage converters. Buck Converters have been used in parallel applications to provide redundancy and higher output powers. There has been research into the control of buck converters connected in parallel and their application in current sharing.

As a result, there have been a number of different arrangements and control schemes developed. The simplest of these is the Master-Slave Current sharing scheme [8]. This involves one converter operating with a voltage control loop, producing an output current. The output current of the master is used to set the target current from the slave converters. The slaves run an internal control loop, similar to that in current mode control, in order to match their output current to some proportion of the master current.

Another control scheme involves the inclusion of Current Balance Controllers [51]. These controllers determine the error between the output current of a converter and its desired proportion of the total output current of the system and then applies a gain to this error. The inputs to the controllers operate off a parallel bus, which represents the total output current. The output of these controllers is then fed used as a negative

feedback to the voltage control loop. This control scheme offers the advantage that converters can be disconnected without shutting off the system. This provides some redundancy, which is particularly useful with batteries.

All control schemes can suffer from instability due to the non-linear nature of switch mode converters. Extensive modelling and mathematical analysis have been performed to predict instabilities and to design effective control loops [8][19][20][21][47]. Instability can be reduced by adjusting, current sharing ratios or the feedback gains of the control loops. Reducing the probability of instability is likely to reduce the performance of the control in terms of transient response and steady state errors. It is a balancing act between performance and stability.

The main difference between the majority of current control schemes and what is needed is that they work on the output current, whereas, the system presented will be working off the converter input current. The schemes presented can easily be modified to accommodate this and could equally be applied to power sharing as apposed to current sharing. These changes are especially easy when the control is all performed on a DSP chip.

Chapter 3 Evaluating Power consumption

3.1 Initial estimates

In order to start designing the power supply it was necessary to get an initial estimate of the power requirements, in terms of both voltage and current. This was extremely difficult so early in the project as most members of the team had very little idea on how their individual section of the humanoid was going to eventually look like.

As was expected the power estimates were far easier to obtain for the supply to the digital electronics than for the motor supply. The process for estimating the digital power requirements mostly involved looking for the maximum power figure on the individual component datasheets. Most boards were quite simple containing only one microprocessor and a few interfacing circuits. Altogether, these used very little power with each of the seven boards using under 300mA each. The only exception to this was the SH4 board, which contained an SH4 but also an FPGA, SRAM, SDRAM, boot loader, Flash memory and various peripheral devices. This board also supplies power to the Camera and to the IPAQ/SH4 interface and in total it was expected that it could consume up to 1A.

Table 3-1 Power Consumption

Device	Number	Voltage (Nominal)	Current (max each A)	Max Power each
IPAQ	1	5	2	10
SH4+camera+interface	1	7.2	1	7
Servo controller	1	7.2	0.5	3.5
Servos	8	7.2	0.75	5.5
Joint Controllers	5	7.2	0.5	2.5
RE 36 motors	15	32	4	120

So in total with the seven digital boards the vision system and the IPAQ the total power requirements was 5A from a 7.2V source. These figures were largely calculated by the people working on the respective areas so they were expected in some cases to be overly pessimistic and in others to be optimistic.

The process to calculate the power needed for the motors was more complex and tedious. The whole process, as with the complete mechanical design was a highly iterative process. First rough calculations were based on the torque required to move an approximated limb. From the calculated torque and expected motor and gearbox, characteristics the required motor current and then expected voltage were calculated. The motor current and voltage along with an expected efficiency for the motor drivers gave the estimated power required for one axis of rotation.

The humanoid has in total 15 high torque axis of rotation. Each axis has different loading characteristics both when standing and during walking. As such, it was difficult to approximate the relative loads of each joint as it depended on the position of the

whole robot and of the final walking algorithm. From what seemed at the time to be pessimistic assumptions, the initial power estimate arrived at was 300W.

The inaccuracies involved in the calculations were known and this was not by any means seen as close to the final figure. As it was required that some work proceed in the design of the power supply this figure was taken with the knowledge that the final result may be twice as high or half the initial estimate.

3.2 Simulator Results

Throughout the entire project, the team used a mechanical simulator to develop both the mechanical design and the walking algorithm [47][18]. The simulator was developed by Dr Gordon Wyeth [52] and is based on the DynaMechs project by Scott McMillan [23]. The simulator is capable of producing torque time profiles for each of the degrees of freedom of the humanoid, with calculations being performed in 200us integrations. Models for the motors were included in the simulator enabling limitations such as the required current limiting to be examined in simulator time. Using the torque data from the simulator and the motor models it was possible to obtain the current and voltage profiles for all the motors.

This was done using a script in Matlab, which multiplied the current by the voltage for each motor, resulting in the instantaneous power profile for each joint. After applying, an efficiency allowance for the drivers and cabling it was possible for the total power consumption versus time to be examined.

The two factors that were most of interest from the power systems point of view were the average power and the peak power. It was clear early on that while the continuous power was relatively high, that the most pressing design issue would be meeting the peak power consumption.

The earliest data from the simulator yielded an average power requirement of 270W with a peak of 450W. As the mechanical design progressed and the actual mass of the limbs became more accurate, the power requirements increased. Throughout the project, the highest that the expected average power reached was over 1kW with peaks of 2kW. This was diagnosed as problems with the simulator models and walking algorithm.

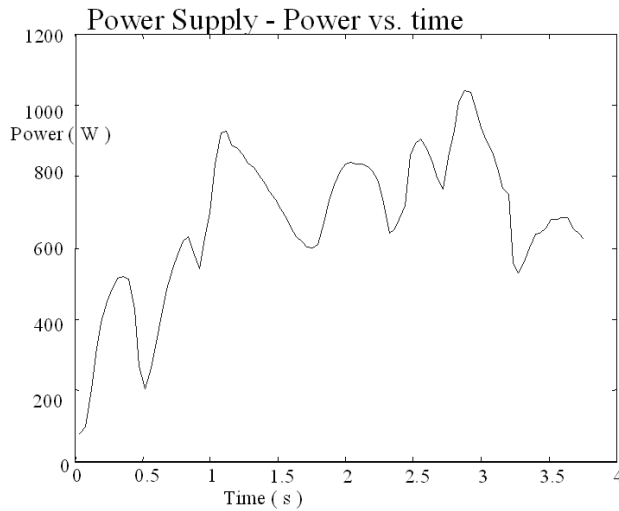


Figure 3-1 Early Simulation of Power Requirements

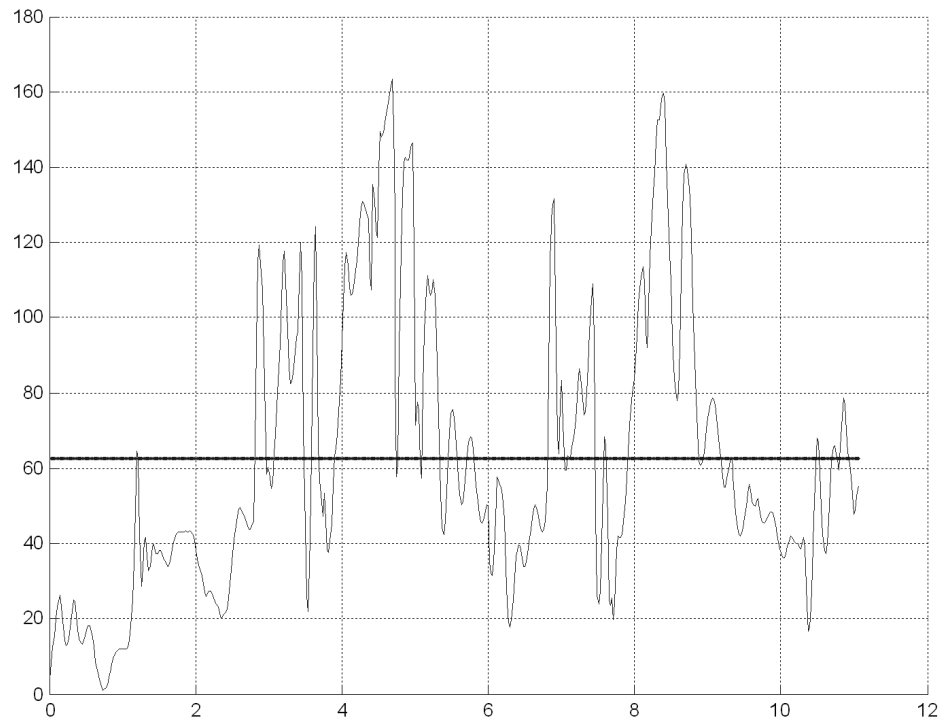


Figure 3-2 Simulation of Power Requirements as of 10/10/2001

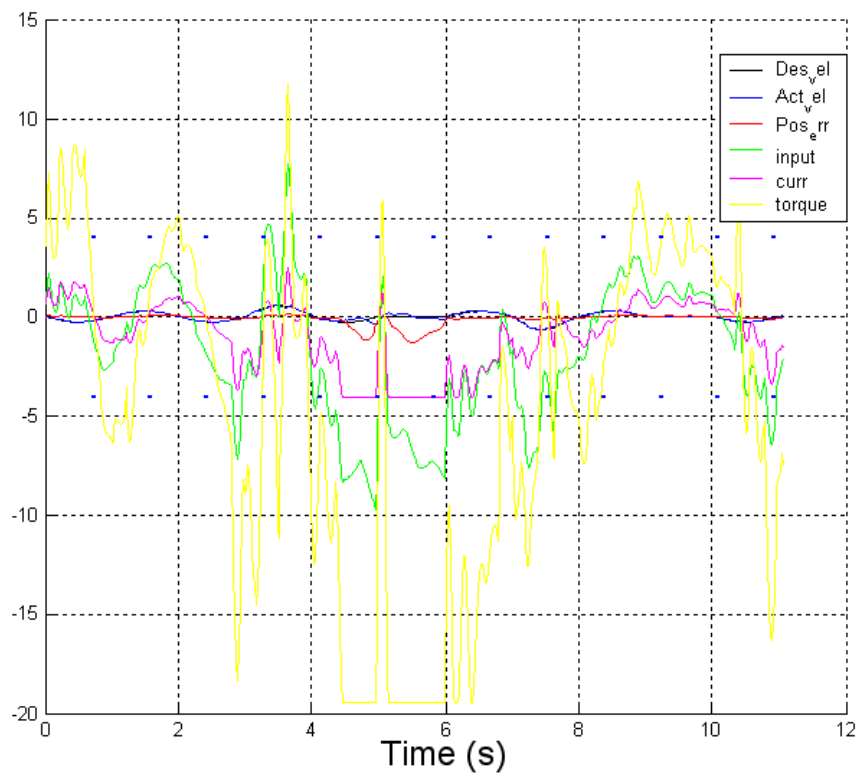
Nevertheless, actual power requirements depend largely on the final weight of limbs, angle of different axis, motor choice and walking algorithm. Over the project, it has become clear that certain walking algorithms can be far more efficient than others can. This highlights the need, that for a humanoid to be truly mobile, it must not only be able to walk but must do so efficiently.

Techniques for reducing torques applied at a joint usually result in lower peak power values from that joint motor. An example is placing springs in the hips, which reduces continuous power when standing but increases the peak power when trying to rotate around the axis compressing the spring. Certain design decisions eventually lead to a trade off between peak and continuous power consumption. From the mechanical point

of view, the peak torque conditions are the biggest design issue as the motors are limited to a continuous current of 1.99A.

This current limit can be avoided by either changing the mechanical design, decreasing weight, or by moving the joint slower. In addition to the continuous current limit, there is also a 4A peak current limit introduced by the motors' H-Bridge drivers.

Below is an example of one of the graphs obtained from the simulator and contains torque, voltage, current and position error traces. From the graph, it is possible to see the effects of the current limiting to 4A and how this limits the torque.



From the above graph, it is clear to see that the current simulator model and walking algorithm produce average and peak power less than what was seen for most of the project.

3.3 Design Requirements

When the first draft of the mechanical design and walking algorithms were produced, the average power required from the supply was 800W with peaks of around 1400W for up to half a second. This data seemed in line with the changing results over the design process and only minor changes in the mechanical design were expected, while the walking algorithm required improvement. The minor changes in the mechanical design and the substantial changes in the walking algorithm led to very little change in the average and peak powers.

For these reasons it was decided that, the 800W average power and 1.4kW peak power would be the preferred design requirements. The humanoid was required to run for 20 minutes and the batteries were required to have a mass under 4kg. From this data, the selected batteries should have a power density greater than 200W/kg and an energy density greater than 67Wh/kg. This data along with the dimension and discharge and safety characteristics of the batteries could be used to determine cell selection.

Within two weeks of the requirements being set, unexpected design changes led to a reduction in expected power consumption. This gave some room in design requirements, which meant that the power supply solution might be able to run for the whole 20 minutes. The revised simulations gave power consumption at under 400W. In the end the required running time was seen as the least important as just getting the humanoid to work would be a significant accomplishment. Therefore, it was decided that the power and weight requirements were the most critical.

With the uncertainty that was still surrounding the actual power consumption, it was decide to stick with the 800W requirement to be on the safe side.

Chapter 4 Power Sources

As can be seen from chapter 2, the advantages of using batteries as the preferred power source outweigh their own disadvantages and the advantages of other power sources. The ease of use, high power and energy density, the ability to recharge, the lack of noise or associated air pollution and availability makes them the most practical choice. This chapter will discuss the different battery chemistries and the reasons behind the selection of the final batteries. It will examine the characteristics of the selected batteries under charge and discharge and discuss how this will affect their use and performance in the humanoid. In addition, information on associated hardware and operation instructions for the batteries will be included

4.1 Battery selection

Three main battery chemistries are practical for use in the humanoid. These include Lithium Ion (LiION), Nickel Metal Hydride (NiMH) and Nickel Cadmium (NiCd). The older of these technologies and still most prevalent is NiCd, but it is increasingly being replaced with NiMH and LiION as their technology improves. Cadmium is a highly toxic heavy metal [6], which if disposed of improperly and not recycled, can be very damaging to the environment. It is for this reason that the NiMH battery has become increasingly popular as it has very similar power and energy characteristics, while being made out of relatively environmentally safe materials. LiION batteries are emerging as a popular chemistry due to their high energy density.

Rechargeable NiCd batteries are available for replacement of most common Primary battery types. They are heavily used in industrial applications such as satellites [46] and consumer applications such as Remote Control Cars, portable radio gear. NiMH has largely been seen as a replacement for NiCds and therefore has many similar applications. NiMH cells have power and energy densities, which are approaching but

generally less than those of NiCd, but offer the advantage of being less toxic due to the lack of the heavy metal Cadmium [6].

LiIONs have a higher energy density, which appeals to portable and low weight systems such as Laptops, camcorders mobile phones and other communication gear. These cells though are limited by their maximum discharge rates usually only at 2C, and if minimally mistreated and they get hot, metallic lithium formed on an electrode, can catch fire causing the battery to burn or even explode [38][45].

While LiION cells have higher energy densities, around twice that of NiCd or NiMH it also comes with an increased safety risk. If misused lithium metal can build up on the electrodes and if heated enough can catch fire leading to a possible explosion. This type of risk is not very practical in robotics so if used, very extensive protection must be incorporated.

With this data and the charge-discharge characteristics presented in battery datasheets, it is possible to start to compare some individual cells. The first two cells that were investigated were the MP1451 LiION cell from Saft Batteries [45] and the P-150AS NiCd cell from Panasonic [36]. Both of these cell types have been used on the Sunshark (a solar powered racing car developed at UQ), and it was possible to obtain some of each of these cells second hand, 16 LiION cells and 20 packs of 32NiCd cells. Another cell that was investigated was a NiMH GP1000AF [7] cell that would be used on the RoboRoos (a robotics team at UQ that competes in the small sized soccer league at RoboCup). The data for these three cells along with some other interesting [XXX] possible cells is shown in the tables below.

Table 2 Battery Properties

Part no	Manufacturer	Chemistry	Capacity		Vnom	Mass	
			Ah	C			
MP 176065	Saft	LiION	5.5		3.6	150.0	
P150As	Panasonic	NiCd	1.5		1.1	27.0	
VR 4D	Saft	NiCd	4.5		1.1	150.0	
HHR150AA	Panasonic	NiMH	1.5		1.1	26.0	
2/3 AF	Gold Peak	NiMH	1.0		1.1	19.0	
CGR18650H	Panasonic	LiION	1.5		3.2	40.0	
Total							
Part no	Power /cell	W/kg	Energy	Wh/kg	no of cells	Mass	
							W
MP 176065	39.6	264.0	19.8	132.0	20.2	3.0	
P150As	5.0	183.3	1.7	61.1	161.6	4.4	
VR 4D	34.7	231.0	5.0	33.0	53.9	8.1	
HHR150AA	3.3	126.9	1.7	63.5	242.4	6.3	
2/3 AF	3.3	173.7	1.1	57.9	242.4	4.6	
CGR18650H	9.6	240.0	4.8	120.0	83.3	3.3	

The table shows the cell properties including mass, nominal voltage and maximum discharge current, in terms of capacity. From these values, it was easy to calculate the power to mass, and the energy to mass densities. From the required specifications of 800W for 20mins(1/3h), it is possible to calculate the number of cells required, as shown below

$$number\ of\ cells = \max \left[\left(\frac{800W}{power\ per\ cell} \right), \left(\frac{800W}{3 \times energy\ per\ cell} \right) \right]$$

As can be easily seen, the LiION cells have higher energy density than the other chemistries, over twice that of NiCd, 130Wh/kg vs. 60Wh/kh. Here the LiIONs also

have a higher power density, which shows the improvement in the state of the technology.

From the calculation of the number of cells required it would only take 20 of the MP 176065 LiION cells to provide the required power, and they could power the humanoid for 30 minutes. It would only weigh 3.0kg and would meet all the specifications required if the cells were handled correctly. However one extreme negative is the cost of \$1800 AUS per set of batteries, and with the desired requirement of four sets this brings the cost of the batteries alone to \$7200. This was outside the budget of the project for this year as we only had 16 of these cells available from Sunshark, not even enough for one set.

Of the NiMH cells shown the 1.0Ah cell from Gold Peak requires the lowest overall mass of 4.6kg to meet both the energy and power requirements. However, it only just meets both of these requirements and at a cost of \$1750 a pack and a total of \$7000 for the 4 sets, again cost becomes a limiting factor.

Of the NiCd cells the P-150AS, from Panasonic has the highest energy density and consequently the lowest total required mass of 4.4kg for one set of batteries. The other NiCd cells all require a total mass that is much greater than allowed for the packs. To meet the energy requirement, 162 cells or 5, 32 cell packs are required. As over 20 of these 32 cell packs were available free, cost was not an issue for these cells.

With the reduction in the simulated power, consumption after the design requirements were set it was decided to relax the requirements so that only four of the 32 cell packs would be used. This meant that the power supply would not be able to operate as long as may be needed depending on the final requirement. The power requirement could still be met as previous use of the batteries in the Sunshark revealed that with sufficient cooling the cells could be pushed to supply up to 6A or 4C, allowing the 800W to be met.

As the running time was not the highest priority, it was decided that the solution of four 32-cell packs was acceptable as it met the more important power and weight requirements. If in the future, the running time becomes a more desirable issue, the packs may with some effort, be reassembled into 40 cell packs to give a 52V pack. As will be seen in the next chapter this would not cause too much of a problem for the designed power supply, but may be a problem for the motor drivers if there is some dramatic failure of the Power Supply, but would probably be an acceptable risk.



Figure 4-1 42V NiCd Battery Packs (3 of)

4.2 Charging requirements

The P-150AS NiCd cells [33] can be trickle charged between 30 and 75mA which would take between 50 and 20 hrs respectively. The option of rapid charge at between 0.75 and 1.5A would take around 1 to 2 hours and is far more appealing for use in a power supply that only lasts 20 minutes. It is intended that a battery charger will be developed to charge the batteries with a current of 1A in about 1.5 hrs.

It is intended that a buck converter be used to set the current through the batteries. This is due to the efficiency of buck converters compared to linear regulators. If a linear regulator was to be used it would have to dissipate around 13W of power per battery during the initial charge time. It is intended that the charger will charge four packs simultaneously and if using linear regulators this would result in over 50W converted to heat.

The datasheet for the cells used indicate that when charging with a current 1.5A, the cell voltage can reach over 1.7V [36]. For a 32-cell pack, this means that the battery voltage during charge can reach over 54V. There is also voltage drop due to the current control circuitry and the resistance in the construction of the pack. It is therefore necessary that the Buck converters be supplied with around 60V to allow a safe operation margin.

The packs can be manually charged using a power supply, which is current limited. The voltage on the battery must be monitored to watch for a peak voltage. When this is reached and the battery voltage begins to fall, the battery is charged. Further charging current will be turned into heat within the battery, raising its temperature dramatically. This charge termination method is known as ΔV cutoff [33] and is the same method that will be used on the chargers.

4.3 Discharge characteristics

The datasheets for the batteries indicate that they can operate at 3C or 4.5A. Testing of the batteries indicate that they can source over 6A while staying within operating temperature limits of -20 to $+65^{\circ}\text{C}$. The nominal impedance of each cell is 14mOhms, giving a total battery resistance, due to cells only, of 0.448 Ohms. Therefore, with 6A current the batteries must be able to dissipate 18W, at 4.5A only 10W.

When fully charged each cell can produce up to 1.4V, giving a battery voltage of 45V and higher when freshly charged. Under a load of 1C, or 1.5A, a fully charged battery will output 43V and under a load of 3C, only 40V. It is expected that the batteries will be running under high load conditions of at least 3C and therefore the output voltage will drop relatively quickly. The battery packs are completely discharged when the voltage reaches 34V under no load.

4.4 Battery PCB and connection

In order to safely and effectively mount the batteries in the humanoid it has been decided to attach a PCB to the end of the batteries. This PCB will contain connectors for Power and temperature along with the batteries fuse.

The batteries have dimensions of 43mm x 65mm x 135mm and have two soldering tabs on the width side 50mm apart. These tabs are bent over and soldered onto the PCB. The batteries fuse is connected between the negative terminal and the power connector. The fuse is located in an Omni Block fuse holder, and will contain a replaceable nanofuse rated at 10A intended to blow for a short circuit of the battery. Placing the fuse on the battery PCB reduces the possibility that a failure occurs before the fuse. The power connector is a 2-pole right angle header (part no 43160-3102) from Molex rated at 19A, more than sufficient (mates with free receptacle part no 44441-2002). The temperature sensor (see section 5.3.2.1 Temperature sensors) and associated resistor are placed on the board and are connected to a two-pole right angle header from Molex (part no 43045-0200, mates with part no 43025-0200). Both of the two connectors are non-reversible, which is critical as a wrongly connected battery could be disastrous.

Chapter 5 Power Supply Hardware

The power supply board is located on the same board as the USB to CAN hardware. The microcontroller is common between the two systems as well as other hardware such as voltage regulators. The positioning of two systems on one board leads to some difficulty with two people having to get the designs to fit together. For detail on the hardware and operation of the USB to CAN interface see Bartek Babel's Undergraduate Thesis 2001[1].

In Chapter 4, it was decided that that four of the 42V battery packs would be used to power the humanoid. The next problem is in what configuration will the batteries be used. There are three options.

The first is that individual batteries power separate control boards. This would result in a minimal amount of required hardware and would remove any problems associated with connecting batteries together. The problem arises when we consider that the boards do not draw a steady power and the power requirements vary from board to board. This would result in individual batteries having very high demands during one part of the walking cycle and very low loads during other times. If the robot were to try to stand on one leg for some time, this would result in one pack being highly stressed over a long time. As a result, batteries would individually have to withstand very high peak loads.

The second option is to place the battery packs in series and to step the voltage down. This is an appealing offer in that it would only involve one converter to control and there would be no problems with current sharing. However, the in series voltages of the packs could be over 200V, if five packs were eventually needed. This poses some safety risks, as this becomes a potentially lethal source. This is not what is needed in a

rapidly moving test environment, which occurs, in a student laboratory. If a failure occurs, or a wire becomes exposed, the implications could be disastrous. With proper protection the circuits could be completely enclosed and the power supply made relatively safe. However, the risk is not worth it when the robot must interact with humans so extensively.

This approach is also limited by the weakest battery in the link. As soon as one battery goes flat or over heats, the supply must turn off. With the batteries used, all being second hand, the potential for batteries to have a wide range of health is high.

The remaining option is to connect the batteries in parallel. This provides a more even loading on each pack, with lower peak load conditions. However, it is affected by the problems of current sharing as described in Chapter 2. The supply can reduce these problems by actively controlling the current from each pack, by the use of Buck converters. As a result, the supply is not, as limited by weaker batteries and can reduce the drain on weaker packs.

It is this last configuration that is used in the power supply. By having the packs in parallel, it is possible to reduce peak loads on individual packs and to keep the voltages at relatively safe levels. This Chapter will discuss the Hardware implementation of the Power supply. It will discuss component selection, design of the PCB along with construction and testing.

5.1 Power supply configuration

In total, the Power supply has six power inputs coming from NiCd battery packs. These consist of two 7.2V batteries for digital and servo supplies and four 42V batteries for the joint motors supply. The GuRoo has a common earth, which means that the grounds on all the controller boards and from the power supply are all connected and at the same voltage. Thus, the power ground and the digital supply ground are the same. This

places some restrictions on the design of the power supply. The biggest being that all control must be done with high side switching as it is not possible to break the ground circuit in any place.

The battery for the digital supply provides unregulated power to the Power supply and USB board and to the electronics boards. The power supply board regulates this supply to 5V to power its own electronics and to provide a regulated 5V to the IPAQ.

The servo supply battery provides motor power to the servo controller board. This board then distributes the power to the individual servos. The output onto the servo supply can be controlled by a MOSFET switch. In the event of a failure, during shutdown or if the robot is about to fall over, it is necessary to be able to turn of this supply.

The board is able to allow active current sharing and current limiting for the 42V packs. This is done by connecting each pack up to a separate Buck converter. These converters are then connected in parallel. By varying the duty cycle of the Buck converters, the proportion of the current from each battery can be adjusted.

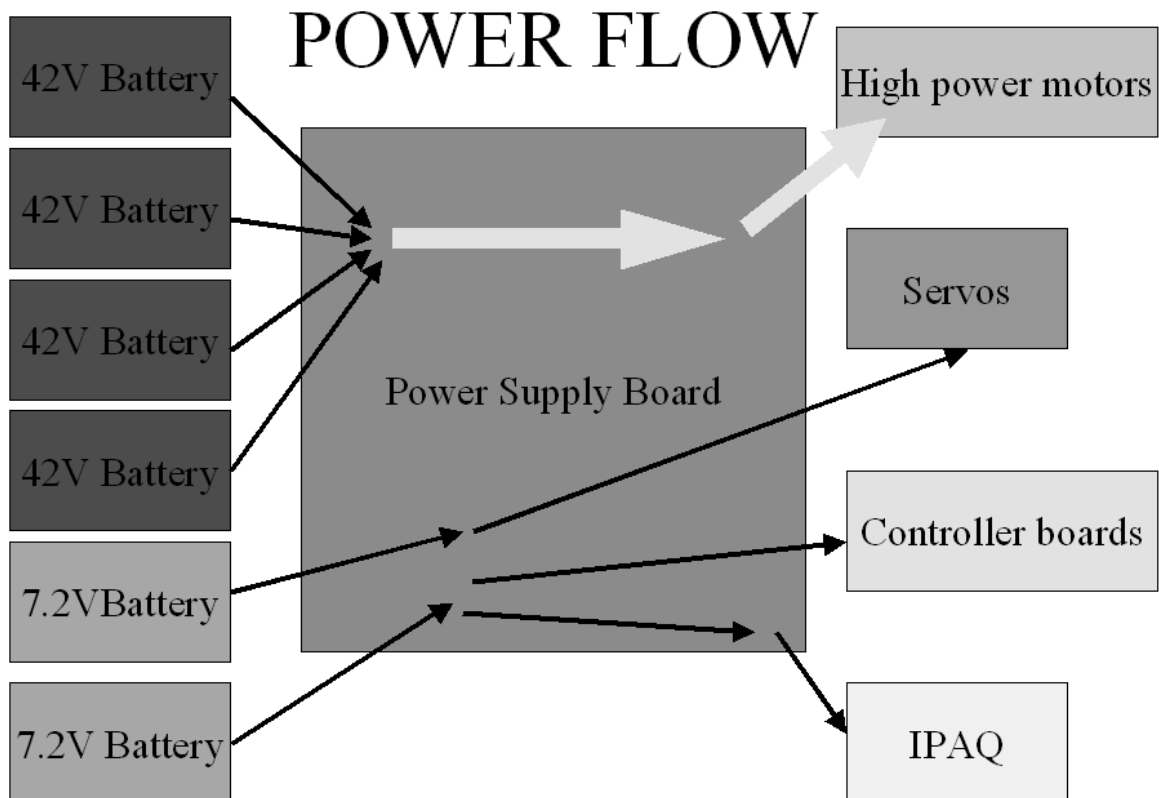


Figure 5-1 Power Flow in the Humanoid

The Buck converters will be connected in parallel using a connector off board. This allows flexibility in the design as it allows the channels to work independently. If it was found that the current sharing was not working adequately the channels could operate independently. It would also be possible to have channels with different output voltages. This would be useful if a range of different controllers or motors were used in the future.

The Power supply is centrally controlled by the TMS320 microcontroller. The TMS measures voltage of all the batteries and, the current in the ground return loops of the 42V batteries are measured. These measurements are sampled by an ADC on the TMS. The two measurements of voltage and current are used to control the output voltage and the current sharing between the Buck converters. The output of each Buck converter can be individually measured as the converters are not connected on board and it is possible that they can run independently of each other.

Each of the four independent Buck converters is controlled by the TMS using four pulse width modulated signals. It is necessary to buffer this signal and to include a MOSFET diver in order to be able to effectively switch the MOSFETs.

5.2 Buck converter design

It is intended that the Buck converters should normally run in CCM. This would enable the current sharing to perform most effectively and will result in less strain on switches and output capacitors. Using the equations in Chapter 2.2.3, it is possible to determine the average output current required to maintain CCM. Using a 100uH inductor, results

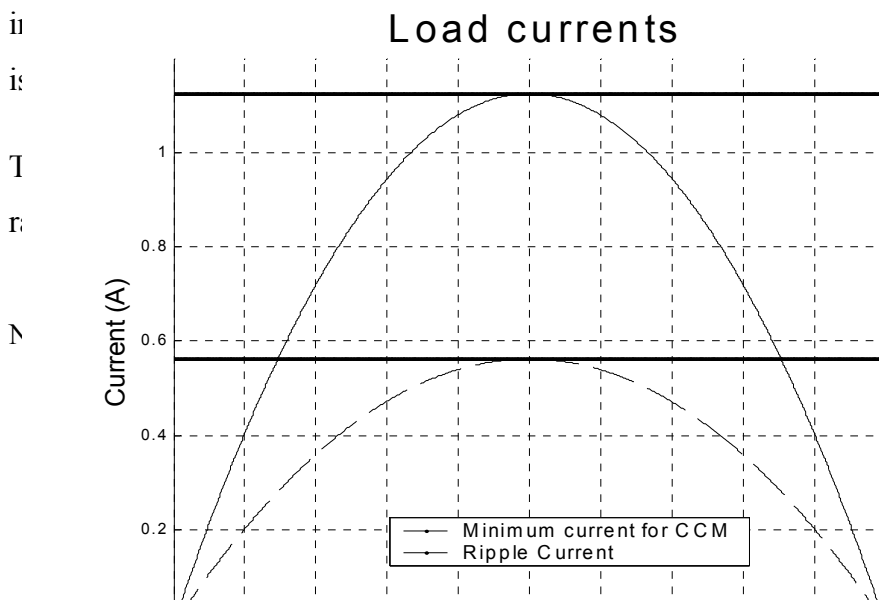


Figure 5-2 Converter Currents

of 50% will result in a 12A load current. The load current will thus vary from 0A to 12A. Together these variables along with the interaction of the parallel converters, leads to a very wide operating conditions. The worst case for the inductor ripple current is when the batteries are fully charged to 45V and the converters are running at 50% duty cycle. From the graph, it is possible to see that the worst ripple current is also at 50% duty cycle and is under 1.2A.

The switching times can be calculated using procedures found in [24]. The switching times will affect the amount of power dissipated during switching. The main factors that affect the switching times are the MOSFET driver, and MOSFET input capacitance. The time between each switch turn on is 10us. The calculated switching times for the MOSFET and driver used is 67ns. This will give in total around 1.5% of a period involved in switching the MOSFET. This leads to a reduction in the duty cycle of the converter, especially when running near 100%.

The capacitor at the output must maintain the voltage, with a reasonably low amount of ripple. It must also be able to handle the ripple current from the inductor of up to 1.2A. Using two 1200uF capacitors, results in a calculated voltage ripple of 0.5mV. In practice, this will be swamped by the voltage drop across the ESR of the capacitor, 40mV, and switching noise. The main reason for choosing such a large capacitor is to be able to supply a large ripple current and to provide more power under high loads.

5.3 Hardware design

The schematic for the complete Power Board is included in Appendix (XXX). In the following sections, there will be a discussion on the selected components and how this impacts on operation. For a detailed look at the connection of the devices on the Board, the schematic should be viewed alongside component datasheets

5.3.1 Buck converter

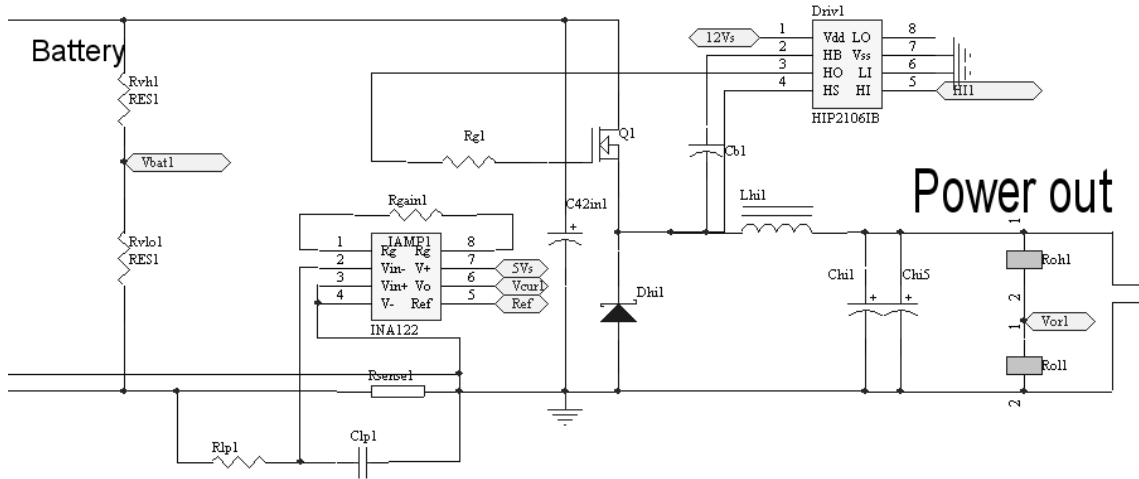


Figure 5-3 Buck Converter Schematic

The Buck converters consist of a number of power electronic devices, which are discussed below. There are a number of properties, besides current handling that must be addressed when designing a SMPS. The devices work together and their interactions will have an impact on switching times and the condition of the output voltage.

5.3.1.1 MOSFETs

A number of device specifications must be considered when selecting a MOSFET for use in a SMPS. The MOSFET must not only be able to handle the required current but must also be able to switch fast enough for the efficient operation of the supply. The current handling capacity of a device is a property of the silicon die, but also of power dissipation hardware. The losses in a MOSFET are made up of on state losses and the switching losses. It was determined that the MOSFET should be able to handle over 12A continuous and that it must switch at 100kHz(see 2.2.3 Buck Converters Theory).

The MOSFET selected is an IRF540 from International Rectifier [16]. The MOSFET has a maximum source to drain voltage of 100V. Which are dependant on the on resistance and the current through the device, and an on state resistance off 44 m Ω . It is rated for a continuous current of 33A, which is dependant on the power dissipation limits.

It is important that the MOSFET can be switched with short transitions between ON and OFF states. These are known as rise and fall times and are largely affected by the gate capacitance. The input gate capacitance for this MOSFET is 2500 pF. Lower gate capacitance leads to faster rise and fall times and a reduction in switching losses. The switching losses in the MOSFET running at 100kHz and 6A were calculated to be 1.1 W. The on state losses were calculated to be under 2W. To dissipate this power, a heatsink with a thermal resistance below 20 °C/W would be needed.

5.3.1.2 MOSFET Drivers

The drivers selected are HIP2106IBHalf Bridge MOSFET drivers from Intersil [13], which come in surface mount SO-8 packages. The driver is rated at 1A peak output current and is designed to drive 1000pF loads at 500kHz. It can operate with Hi side input voltage of up to 100V. The driver is powered from the 12V supply rail.

The driver uses a bootstrap capacitor connected from the high side MOSFET source to the high driver power supply and through a bootstrap diode to the chips 12V supply. When the high side source is connected to ground by the low side switch, current flows through the diode, charging the capacitor. When the driver starts to turn on the high side MOSFET, the voltage of the source starts to rise and the whole high side driver and capacitor with 12 V across it starts to float as the diode becomes reverse biased. This 12V across the capacitor powers the high side driver.

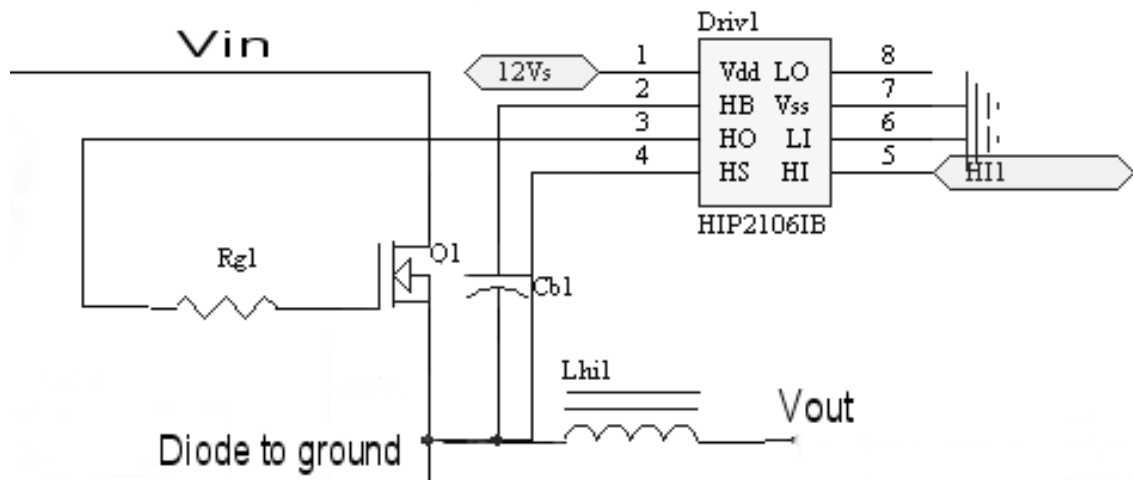


Figure 5-4 MOSFET Driver

When selecting the bootstrap capacitor it should be greater than the gate capacitance of the MOSFET by around four times. This is to give the driver enough power to run over a switch period. If the capacitor is too large, it may not have enough time to charge when the source is pulled low. For these reasons, a ceramic surface mount 10nF capacitor was chosen and was found to work well.

The driver has an output resistance of 3Ω and to limit the current to 1A it is necessary to insert a 9Ω gate resistor. Inductance in the tracks increases the impedance and allows a lower gate resistance to be used. This inductance and the gate capacitance, form an LC circuit, which could start to oscillate. The gate resistor helps to prevent oscillations and can be increased to prevent them from occurring.

The driver has undervoltage detection circuits with a threshold around 7V. When an undervoltage is detected, both the low and high side outputs are forced low, turning off the MOSFETS. This property is used as part of the emergency shutdown circuit.

5.3.1.3 Signal Buffers

The inputs for the MOSFET drivers are CMOS and therefore have a threshold half way between the two supply rails, in this case 6V. In order to convert the PWM signals from the 0-5V TTL signals from TMS to the 12V CMOS, a comparator driven from 12 V is used. Fast switching is needed, as at 100kHz the whole period is only 10us so we need delays will add up, limiting the PWM resolution. A LM319N dual comparator from National Semiconductor [26] was chosen. The comparator has a stated response time of 150ns for $V_s = \pm 15V$. In practice, with $V_s = 12V$, it is higher than this. The output has an uncommitted collector and a 3k pull up resistor from the output to the 12V supply is needed. The threshold for the comparator is set using a 4.7k and 22k resistor as a voltage divider to give 2.1 V. In hindsight, it would have been more effective to use another MOSFET driver, with TTL inputs that converts to 12V CMOS, such as an ICL7667. These drivers are already setup for the fast response times and the correct thresholds, including input hysteresis, which is lacking in the comparator setup.

5.3.1.4 Diodes

The diode selected for use in the buck converter is BYV32E200 diode from Phillips [41]. This comes with two diodes in TO-220 package with the cathodes of the diodes connected to the middle pin. These have a reverse voltage rating of 200V and an average forward current limit of 20A with both diodes conducting. The largest power loss in a diode is due to the forward voltage drop. A diode with a low voltage drop, such as schottky diodes (0.35V), would have increased the efficiency of the supply and reduce the heat sink requirements. The diodes selected unfortunately have a forward voltage drop of 0.85V. The higher voltage is a trade-off for higher current capacity and reverse voltage rating. At an average current of 6A, the diodes would dissipate around 6W, which would require a heat sink of 10°C/W.

When the MOSFET turns on, the diode does not immediately stop conducting as it takes time for carriers to be swept out of the junction. This leads to a time, known as reverse recovery time, when the diode is conducting current in the reverse direction, wasting power. It is necessary to minimize this when selecting diodes. The BYV32EB has a reverse recovery time of around 25ns, which is comparable to the switching time of the MOSFET.

5.3.1.5 Inductors

The inductors are 100uH bobbin type from C&D Technologies (part no 14 104 78). The inductors have a DC resistance of 40mΩ and a maximum RMS current of 7.8A. From the expected RMS current, the inductor would be dissipating 3W of power. The inductors are 32.4 mm in diameter and 21.8 mm high. They are the heaviest of the components on the board and have a mass of (XXX) g. It may be possible in the future to find smaller and lighter inductors to reduce the size and weight of the power supply. Inductors with a lower resistance and higher current handling will improve the efficiency and power output. A possible future supplier could include Coilcraft, which have inductors that are smaller in size and weight.

5.3.1.6 Capacitors

The capacitors used in the buck converters are 1200uF 63V FC series electrolytics from Panasonic (part no EEUFC1J122) [32]. The expected output voltages of the Buck converters are 40V. However, voltage transients due to switching will require that the capacitors can handle significantly higher voltages than this. The capacitors have an allowable ripple current of 2.95A and an equivalent series resistance of 32mΩ. A high ESR coupled with high ripple currents will lead to high power dissipation in the capacitor. Therefore, the low ESR is necessary to keep the capacitors from overheating and venting electrolyte. The capacitors are physically quite large, being 31.5mm high, and having a diameter of 18mm.

5.3.1.7 Current Sensors

The current in the ground return loop to each of the 42V batteries can also be measured. This was done by placing a 0.005R resistor in the circuit and by measuring and amplifying the voltage produced across the resistor using an instrumentation amplifier (INA122UA)[2]. This differential amplifier uses level shifting circuitry that allows voltage inputs 0.1V below GND. The amplifier requires only one resistor, which is used to set the gain. The positive input is connected to ground and the negative input is connected via an RC low pass filter to the other side of the sense resistor. The filter helps to smooth the 100kHz ripple from the switching.

In order to be able to sense positive and negative currents, it is necessary to offset the outputs by applying a reference voltage to the Amplifier. An LM311 amplifier with an internal voltage reference is used to provide an adjustable voltage reference.

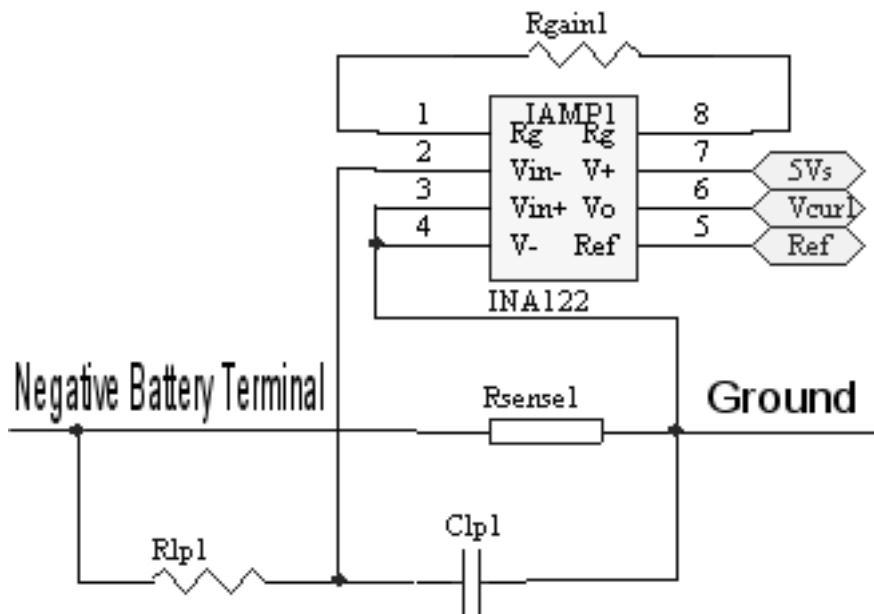


Figure 5-5 Current Sensor

5.3.2 Measurements

5.3.2.1 Temperature sensors

The measuring of the temperature of each battery is accomplished using an LM35CAZ [28] (TO-92 package) in a two-wire configuration. The temperature is converted from a voltage signal into a current signal by tying the output pin of the LM35 through a 200 Ω resistor to its' negative rail. The voltage across the resistor produces a current in the negative rail proportional to temperature. This current is then transported back to the main power board were it is converts back from a current into a voltage by passing it through another 200 Ω resistor. The LM35 produces a change of 10mV per degree Celsius, which will correspond to 50uA per degree Celsius. The LM35CAZ has a claimed accuracy of +/- 1.5 $^{\circ}$ C, which is accurate enough for measuring battery temperatures.

5.3.2.2 Voltage measurement

In order to assess the state of the batteries for control and safety purposes it is necessary to measure the battery voltage. On the 42V packs this is accomplished using a simple voltage divider (22k and a less than 1.7k resistor) to take the voltage from a range of 70V down to the ADC measuring range of 0-5V. The extra margin provided by the 70V will provide some protection for the ADC or proceeding buffers from an over voltage placed on the input of power board, from either an incorrectly setup laboratory power supply or from voltage transients. Similarly, the 7.2V packs are step down from a range of 10V. The voltage on the output of each Buck converter is similarly measured.

5.3.2.3 Multiplexers

There are only eight analogue to digital converter ports on the TMS and it is therefore necessary to use a multiplexer to add the extra capacity necessary to measure the 21 channels needed. To accomplish this two eight channel 74HCT4051D [42] multiplexers from Phillips are used. These have on resistances of 80Ω and switching times of 25ns. The outputs of the two multiplexers are joined together and the enable pins of the multiplexers will be used to select between the two. The outputs of the multiplexers go to high impedance when the enable pin is low. The address pins of the two are connected and controlled by the TMS.

5.3.2.4 Buffer Amplifiers

The ADC ports have an input capacitance of 30pF [49] and if there is an input of 80Ω from the multiplexers, this will lead to a slow response time when the multiplexer channels are changed. In order to reduce this effect a signal buffer is needed. This consists of an opamp with unity gain. It is important that the buffer itself have a reasonable slew rate and have a good output voltage range. The LMC6801AI amplifier from National Semiconductor [29] has a slew rate of $0.6\text{V}/\mu\text{s}$ and an output range of 0.63V to 4.2 V. With the 10bit ADC this gives a possible 730 voltage levels, or better than 0.2% precision if the input voltages are within the suitable range. The slew rate provides some problem as to change by 3.5V it may take up to 10us to settle within a low error. Each channel will be read once every millisecond, so with 14 channels coming through the buffer, this gives $70\mu\text{s}$ for each reading. This should allow enough time for the multiplexer and buffer to stabilize the voltage at the ADC input.

5.3.3 Power regulators

5.3.3.1 5V Regulator

The 5V regulator has to supply the TMS chip and USB hardware on the Power Board, as well as an external connection to the IPAQ. It is required that the Regulator supply up to 3A so the LM1804 from National Semiconductor was deemed sufficient [25]. This has a claimed output voltage of between 4.9 and 5.1V with a 20mV load regulation. This voltage range is sufficient for the IPAQ and onboard digital electronics but may provide some difficulties for the ADC converter reference, which is powered off the 5V rail. When the Regulator is running under a full load of 2.5A, it will need to dissipate 8.5W ($P = (8.4V - 5V) \times 2.5A = 8.5W$). The device has a junction to case resistance of 2.7K/W, a maximum junction temperature of 150°C and with an ambient temperature of 50°C, the thermal resistance of the case to ambient must be less than 9K/W. This requires a decent size heat sink of around 8K/W, to be reliable.

5.3.3.2 12 Boost Regulator

In order to power the MOSFET drivers it is necessary to produce a 12V supply rail. This is accomplished using a simple switch mode boost converter from National Semiconductor. The LM2586-12 can be used in a boost topology to produce a regulated 12V from the 7.2V battery input as shown below (for a description of Boost see [24]). The regulator requires minimal support circuitry

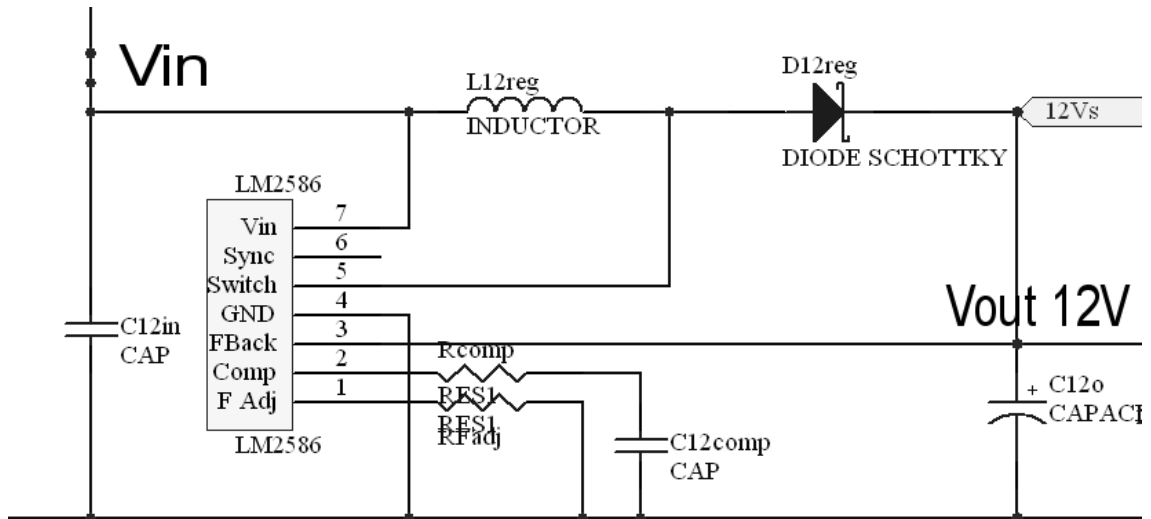


Figure 5-6 12V Boost Converter

The circuit uses a 470 μ F capacitor on the input and output, which are rated at 25V and have a maximum ripple current of 1A. The diode used in this circuit is 6CWQ03FN schottky diode from International rectifier [14]. The low forward voltage drop, 0.35V, and the high current handling, 7A, make this diode suitable for the regulator. The inductor is a 4.7 μ H from Panasonic (part no ELC10D4R7E)[35]. The inductor has a resistance of 19m Ω .

The power supplied to the regulator flows through a fuse and then travels through a connector to the emergency shutdown switch. If the switch is released, power is cut to the 12V regulator. This in turn cuts power to the MOSFET drivers, which will turn off the MOSFETs, effectively switching off the Power supply.

5.3.4 Servo Supply

It is necessary to be able to turn off the supply to the servomotors. This is in case of a collapse of the motors or to just turn off the humanoid. To do this a MOSFET switch

needed to be placed on the Power supply board. The switch would be controlled by the TMS chip and would be turned off if there was a fault, or for shutdown. The switch would need to be in the high side as there is a common ground in the humanoid, including the servo controller board.

The inclusion was a last minute request when it was realized that the servo controller was lacking in this feature. The switch chosen was an IPS5451 [15] from International Rectifier. This has its own charge pump circuitry to provide the necessary gate voltage to turn on the MOSFET. The MOSFET has an on resistance of $30\text{m}\Omega$ and is capable of carrying 14A continuously, depending on the heatsink. At the maximum expected output current of 5.5A the switch would need to dissipate 950mW of power. With a thermal resistance, junction to ambient of $55^\circ\text{C}/\text{W}$ this would allow the device to operate without a heatsink.

5.3.5 TMS320F243

The microcontroller used throughout humanoid was the TMS320F243 16 bit Digital Signals Processor from Texas Instruments [49]. In total, there are seven TMS chips used, 5 on the joint controllers, 1 on the servo controller and 1 on the power/USB board. Each of these chips connect back to the IPAQ through the CAN network and CAN to USB bridge through the power boards TMS chip.

The TMS chip is a 20MHz, 16-bit processor that has 8kB of internal flash memory and 368 bytes of data RAM. The chip is able to be in circuit programmed and it is therefore possible to use a surface mount chip.

The TMS has eight PWM channels, six of which are combined into three compare units. In total, this leaves five independent channels that can be used for the power supply. The first three are part of the compare units, while the last two can operate of one of two

general purpose timers. The three channels from the compare units and one of the other channels are used to drive the individual buck converters.

The TMS has eight analogue to digital converter (ADC) channels. These are capable of conversion times less than $1\mu\text{s}$. This allows up to one million conversions a second. With 21 channels being read at most 1000 times a second, this is faster than needed. The conversion time does come into play when sampling the readings from the multiplexers. This is due to the long time for these circuits to switch and stabilize. The short conversion time means that the ADC does not add significant time needed to stabilize a reading.

5.4 PCB layout

The PCB is a 4-layer board measuring 6 by 8 inches. When fully populated the board should have a height which is under 5cm. An internal layer was used as a continuous ground throughout the board in order to reduce noise (see Appendix).

The main digital circuits and more sensitive analogue circuitry were placed on the underside of the board in an effort to reduced electromagnetic interference from the power electronics. The USB and microcontroller connectors were supposed to be on the top layer of the board to reduce overall height but stuff up resulted in

From the picture above, all power inputs are on the left of the board with all outputs on the right. The four buck converters were set up as modules with similar layouts so that it was easier to place components and route tracks. An extensive use of internal planes for the high voltage power connections, allowed the use of track between 10-30mm wide. An effort was made to make all tracks as wide as possible to reduce resistance and inductance.

Due to wide power tracks and the left to right power flow, it was difficult to route signal tracks which all travel top to bottom from the microcontroller. As a result, signal connections tended to have to weave their way from the top to bottom layer and back again. This is especial noticeable in the address pins for the multiplexers.

5.5 Construction and testing

There was quite some delay between when the PCB boards came back and when the controller group got the PCB working. To program the boards it is necessary to load the serial boot loader into the memory using the JTAG interface. Once this is done you should then use the serial port to programme the TMS serially, making sure it loads the boot loader back into memory.

We had been trying to wait until this was done as it was seen that the TMS chip was the most delicate on the board and that it was the most likely to have some problem with some of its circuits. Due to two people using the same board, it was decided that Bartek should try to get the TMS and USB hardware working on one board and then once this was working then populate another board with a second lot of components. Before the TMS on the power board was working fully it was found necessary to start to place some of the bulky Power electronics onto the board.

First placed were the current sense resistor and the Instrumentation amplifier and voltage reference generator. These were small surface mount components so placing this should not have hampered placing other digital components on the board. However, after getting one set of the current sensors working correctly there was still no progress on the TMS booting. It was decide to go ahead and place power components on the board. In the end, this did not hamper placing the TMS chip on, as by good design it was placed away from the power components and on the underside of the board.

The first components to be placed on the board were those of the 12V boost regulator, which would be used to drive the MOSFET drivers, comparators and the temperature sensors. This was tested for an input voltage range of 5-10V and was found to work effectively. Under a test load of 1A, it produced a stable output of 12.3V. The 0.3V inaccuracy is not important and will not affect any components. There was an undetectable amount of switching noise from the converter, on either the 12V rail or the 5V rail.

Next, one of the MOSFET and associated driver were placed on the board. The MOSFET was tested with switching frequencies up to 200kHz and was found to work effectively. The inductors and capacitors of this buck converter were placed on the board and the converter was tested.

A wire wound variable resistor, in a two by 70 Ω configuration, was used as a load for the buck converter. Two channels of a laboratory power supply in series were used to provide input voltages up to 60V, with input currents up to 3A. A signal generator was setup with a 100kHz 12V square wave and was used as an input to the MOSFET driver. This test setup was used to evaluate the Buck converter in operation by itself. For detailed results, see chapter 7. The Buck converter was found to work very effectively and the output voltage could be adjusted by varying the duty cycle on the signal generator.

The controller boards finally began to show some life. From this, fears that the circuits around the TMS were wrong were removed. It was then possible to get the TMS soldered on the board and to finally get the controller programming. A number of problems arose on the board. The point where the output of the 5V regulator connects to the Vcc plane under the controller section of the board, was damaged when a component was placed on. It was necessary to run a hook-up wire from here to another via that connected to the plane. The moral being, do not rely on a component to connect directly to a plane unless it is very solid.

The TMS worked correctly and it was possible to control the output of the Buck converter using the TMS chip. Initial problems were encountered with disabling the power protection interrupts, in the software. Once fixed the PWM waveform observed was clear for a wide range of duty cycles at 100kHz. The LM319 signal buffers worked correctly once the pull-up resistor was included.

The hardware after some minor corrections was deemed to work as desired however future improvements could still be made. This is particularly evident in the amount of free space visible on the board. It was noted that direct connection to the Power planes such as GND makes it difficult to solder as the heat was dissipated quickly. The benefit of lower resistance of direct connections may not offset this in future revisions.

5.6 Wiring harness

The wiring harness must deliver four types of power to 10 different objects. While doing this, the harness is required to be as reliable and simple as possible. As the route on which the wire must travel, is moving, it is necessary that the wires remain as flexible as possible. The wire selected should be multicore with as many strands as possible. In addition, the insulation should be flexible, light, and resistant to abrasion and heat. The wire selected for the connecting to the motors and the wire to the motor controllers is called Flexiplast and is from MC. The wire for the motors is 0.5mm^2 in conductor area and is rated at 10 A. It has 129 strands per conductor with an outside diameter of 2.1mm. The wire for the motor controller supply is 2.5mm^2 in conductor area and is rated at 32 A. It has 651 strands per conductor with an outside diameter of 3.6mm. Both of these wires were found to be very flexible and light.

It was possible to find a flexible shielded cable containing seven multicore wires. This seemed ideal to carry both the CAN and the digital supply. The CAN network is in a chain and it requires two wires to and from every controller. The shielding offered by the cable will help to reduce errors on the CAN network as noise from motors and

drivers in the humanoid would be quite high. The cable is made by Deltron, is called GAC-7, and has an outside diameter of 6mm.

5.7 Mounting the Power System

It is intended that the power board along with the batteries be placed in the torso of the completed humanoid [50]. The board is centralized allowing easy distribution of power and the CAN to the different electronics boards. The limited space in the torso made it difficult to mount the supply, so future revisions should try to reduce the size of the board.

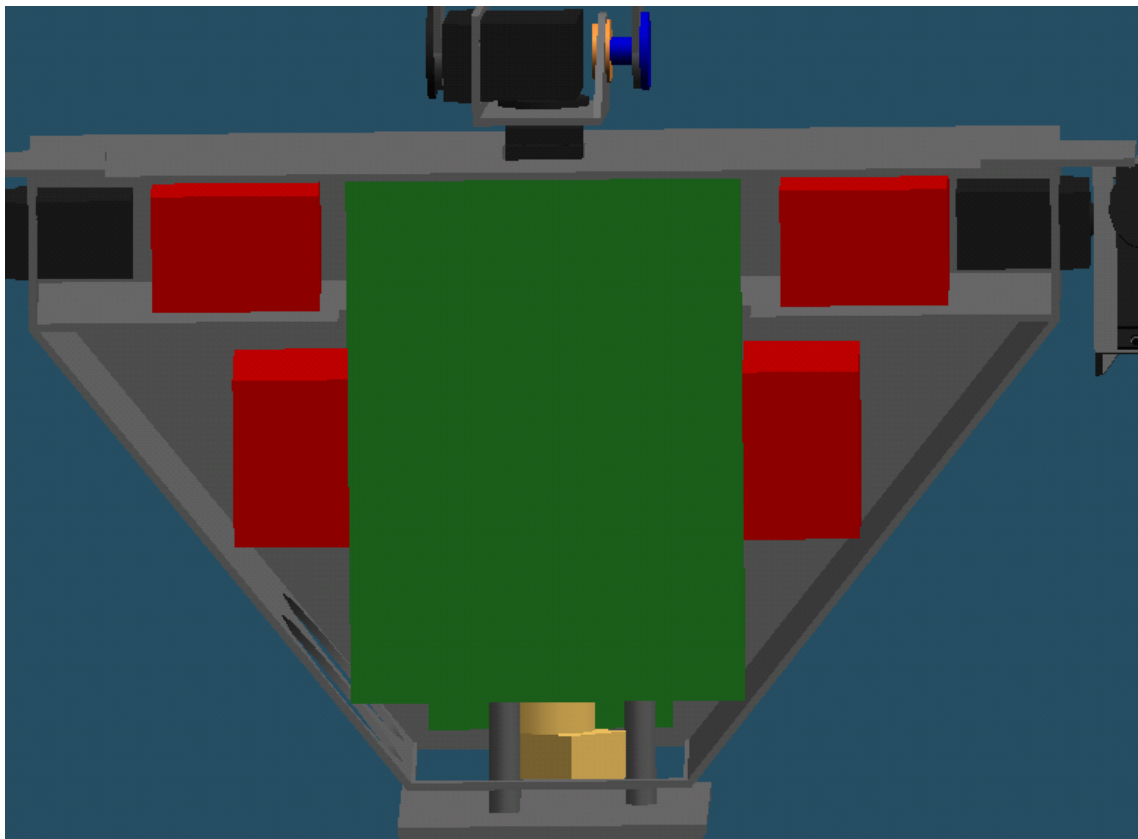


Figure 5-7 GuRoo Mounting of Power System [50]

Chapter 6 Control of the Power Supply

This chapter will discuss the major control structures for the operation of the supply. These are divided into the Buck converter control loops and the Algorithm Controller. It will list the requirements of the control scheme and problems that must be addressed for control loops to work effectively. All the control processes are run on the TMS chip on board the power supply, but the supply is able to communicate to the rest of the robot.

As the power supply board is connected to the IPAQ through the USB port, it becomes possible for the condition of the power supply to influence the operation of the GuRoo. If the temperatures of all the packs are reaching dangerous levels, the power board can request that the GuRoo use less power. This may result in a need to stand still for a while, so that the batteries can cool. If the load on the power supply is reaching a pre-described or calculated maximum, the IPAQ can be asked to slow movements of the robot down, or could be alerted to the possibility of a fault.

The communication can work in reverse, with the IPAQ issuing commands for the power supply to shutdown or turn on. It will be necessary for some method to turn off the GuRoo especially if there is a problem. Similarly, when starting the GuRoo it may be beneficial to check that all the electronics are working before power is supplied to the motor drivers.

6.1 Requirements of control

The main aim behind the control scheme used, is to protect the batteries and hence the humanoid from damage. Second to this, is to efficiently provide adequate power for as long as possible. The control scheme will regulate the relative power loads on packs

depending on their voltage and temperature. It must also be able to disconnect batteries by stopping the MOSFETs from switching on.

The batteries must be protected from over discharge as this causes permanent damage. The controller will disconnect a battery, when it reaches the set discharged voltage. Due to the intrinsic diode found in MOSFETs, the output voltage of the other converters must be kept below that of the lowest battery. Otherwise, the diode will conduct and reverse biasing will occur.

Batteries with a higher voltage would normally indicate a higher state of charge. As a result, it would be beneficial to apply a heavier load to these supplies. This will help to balance out the state of charge of the packs leading to a longer operation time.

The batteries have a working temperature from -20 to $+65^{\circ}\text{C}$. It is not likely that the GuRoo will be operated in sub zero conditions but it is highly possible that the batteries could overheat. The temperature of the batteries will be affected by the amount of power drawn. It will also be affected by the other conditions such as room temperature, heat dissipation of motors, cooling mechanisms and whether the humanoid is in direct sunlight. When one pack has a temperature higher than the others, the controller should start to reduce the load on this pack. The closer the temperature is to the cut off, of around 55°C , the greater the reduction in load, until the pack is disconnected.

In order for the power supply to be able to output the maximum power possible, it is necessary that the current from each source can be controlled. The problems with parallel supplies described in chapter 2 require an algorithm to that controls the currents. This means that if a converter is approaching the current limit then the control algorithm will reduce its output by lowering the duty cycle of the buck converter.

The control scheme used will be able to set the ratio of a converters current to the total output current. The scheme will change the ratios of the currents dependant on the sources voltages and their temperature in order to ensure best operation of the supply.

6.2 Power Proportioning Algorithm

The Power Proportioning Algorithm is used to set the proportion of the total power that each battery is supplying. The algorithm does not need to be executed very frequently, 10This is slower than the pulse-by-pulse control performed by analogue circuits, but the output voltage is not critical as the long-term performance of balancing power is more important.

Control diagram

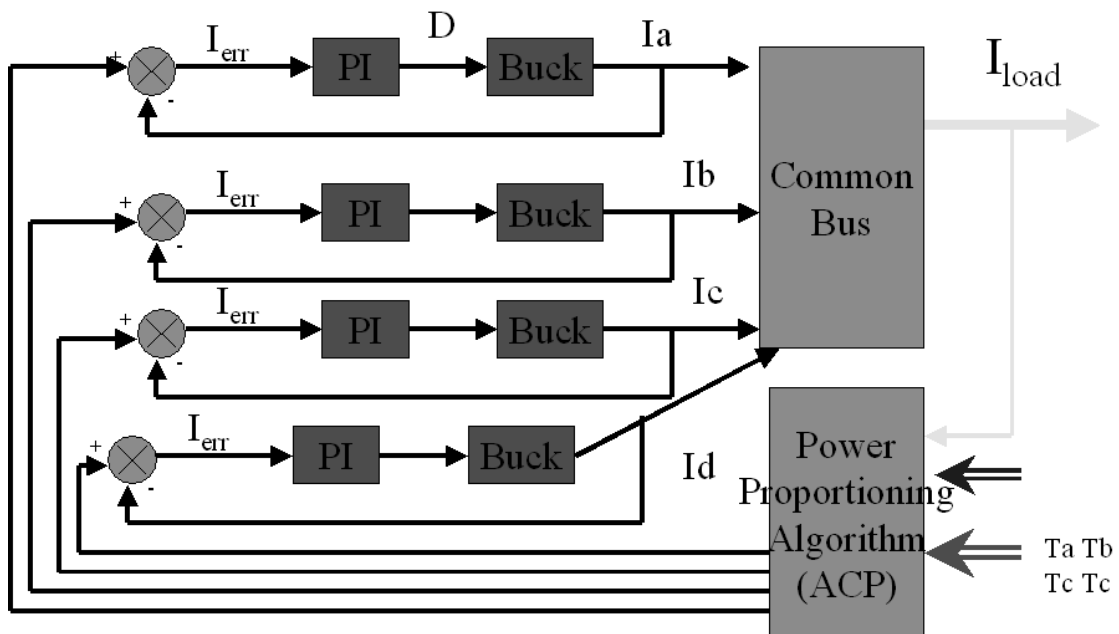


Figure 6-1 Control Diagram

Below is a step through of the algorithm used to set the inputs to the buck converter control loops. This will run once, before every control loop execution.

Control Algorithm

Step 1 Check if a source has exceeded peak operational temperature or peak current. If so, then shutdown the converter for that source. This corresponds to setting the source's weight to zero.

Step 2 Check output voltage for fault. If $V_{out} \ll V_{set}$, if so raise alarm. Calculate V_{set} from lowest battery voltage, eg $V_{set} = V_{lowest} - 5V$;

Step 3 Calculate total powers coming from all the sources

$$P_{total} = \sum_{n=1}^4 V_n I_n$$

Step 4 Calculate the charge state of each pack using approximation curves.

Step 5 Calculate the power capacity of each source.

$$P_{n, capacity} = \text{Charge state} \times \frac{(T_n - T_{room})}{T_n} \times \frac{(I_{set} - I_n)}{I_{set}}$$

Step 6 Calculate weight by dividing source capacity by total capacity.

$$W_n = \frac{P_{n, capacity}}{\sum_{n=1}^4 P_{n, capacity}}$$

Step 7 Report Power consumption as a proportion of maximum possible output power to the IPAQ. Report any warnings and the conditions of the batteries.

6.3 Buck converter control

The control loops will be run at 1kHz. This is slower than the pulse-by-pulse control performed by analogue circuits, but the output voltage is not critical as the long-term

performance of balancing power is more important. The controller contains a PID compensator, which has inputs from three control loops.

The first is the voltage feedback loop which calculates the error between the output voltage, and that set by the algorithm. This loop tries to maintain the output voltage of all converters as high as possible.

The second is the temperature control loop, which will lower the output of a battery when the temperature rises. As this is done on every battery, if one battery is hotter than the others, its output will be lowered compared with the rest.

The third is the power balance controller. The controller first calculates the total power drawn from all units. The weights generated by the Power Proportioning algorithm are multiplied by the total power drawn from each source to determine the set power. The set current is calculated by dividing the set power by the battery voltage. This is compared with the actual current and the error multiplied by a gain and fed to the compensator

The input from all three loops is fed into the PID compensator. The output of the compensator is the on time, in TMS clock cycles, of the PWM signal. This signal must be limited to between 0 and 200, which is the PWM period.

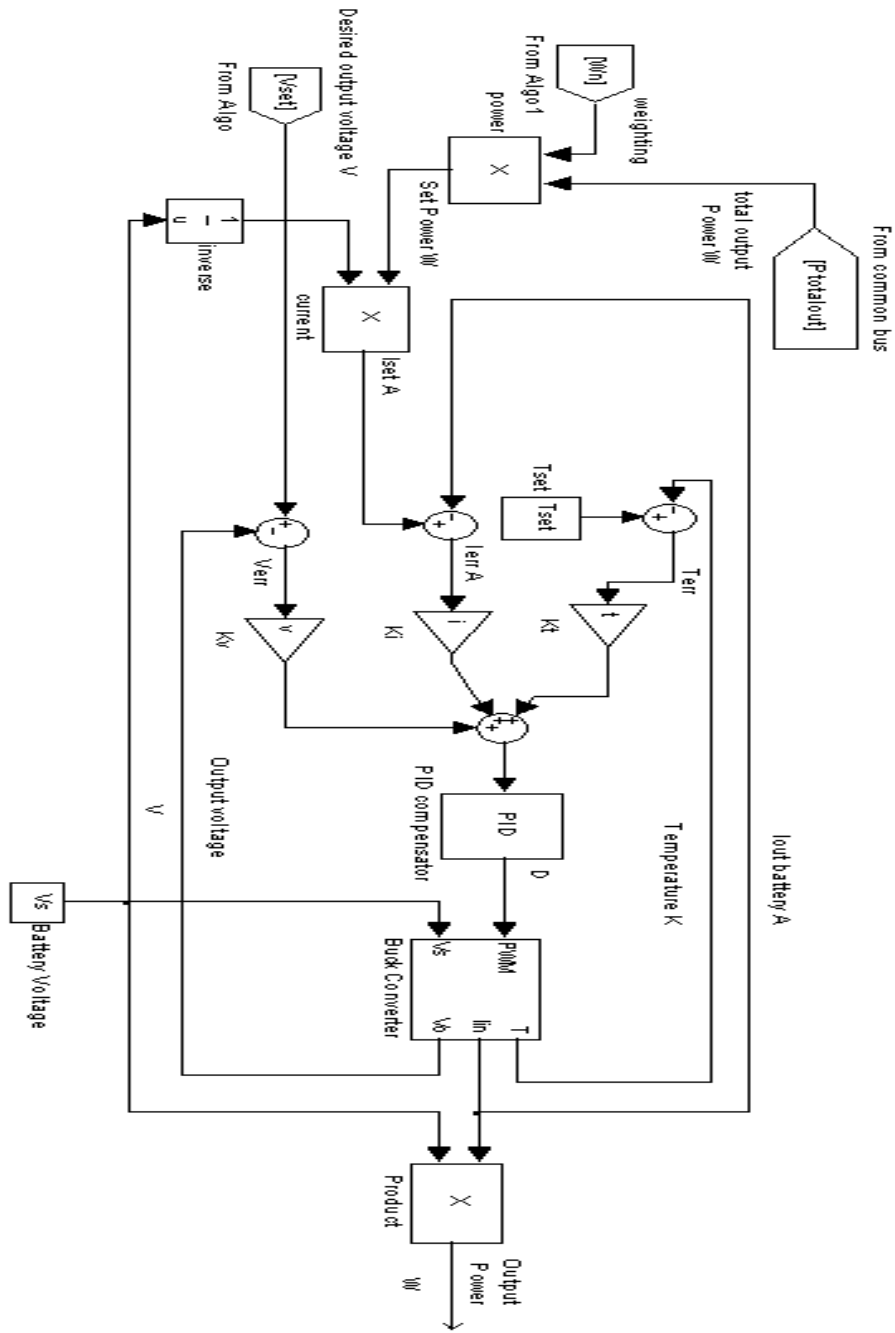


Figure 6-2 Control diagram for Buck Converters

6.4 Avoiding instability

Converters can go unstable and start to oscillate, due to line or load transients. In the case of parallel systems, the line transient can be from another converter. For the power supply, probable conditions include; starting the supply, powering up the motors on the GuRoo, motor start-ups such as lifting a leg or the power supply disconnecting a battery.

Supply startup problems can be limited by soft startup, where the duty ratio is gradually increased to the operating values. Instabilities caused by line/load transients, can be minimized by the selection of the controller gains. Stable gains usually give slower response times. If batteries are disconnected gradually, over 100 or so ms, then the supply is less likely to go unstable.

Prevention is important and good control loop design, modelling and testing, can remove many sources of instability. However, the most important point is to be able to recognise when critical instability, such as oscillations or chaotic outputs, are occurring. Once it is discovered that something is wrong, the supply can be reset, or the control loop gains could be lowered.

Chapter 7 Results

The second hand 42V NiCd batteries from Sunshark were charged and discharged to test if they were still useable. All the batteries tested were useable, and most were in good condition. The average voltage on the batteries was observed to be 44.5V after charging, dropping to between 42 and 44V after standing for over a day. Under discharge, the battery was tested with continuous currents of up to 4.5A and was found to become only moderately warm. The batteries were also tested under peak loads of 6A for a couple of minutes and did not over heat the packs.

Currently one full Buck converter has been assembled onto the Power board. In addition, the TMS and the analogue circuits, such as the voltage reference current sensors and signal drivers are installed.

The TMS chip is booting and can be serial programmed on board. The TMS has been used to produce PWM frequencies up to 100kHz. Programs that change the Duty cycle of the PWM signal over time, have been used to validate the operation of the Buck converter.

The Buck Converter has been run at 100kHz, very successfully. The switching times for the MOSFET, were measured at around 100ns, depending on temperature. The output had voltage ripples of around 100mV, but switching transients of 5V were visible. It may be advantageous to add snubber circuits around the diode and MOSFET to reduce the amplitude of these spikes.

The efficiency of the converter running with 3A load at 30V output was calculated from experimental results, to be almost 95%. This is very good and is in part due to the high voltage of the converter. The power drop due to the diode is proportional to current, so

the higher voltage the converter, the lower a percentage of the input power the diode loss is. This efficiency is evident by the fact that only the diode starts to become warm, under a heavy load and load duty cycles.

Booth the 5V and 12V regulators were tested under full load conditions and were found to work effectively. Neither the 12V boost regulator or the buck converters, introduced appreciable noise onto the 5V rail. Signal integrity from sensors and from drive signals was much better than expected. Tracks that run on the underside of the board had no noise detectable by an oscilloscope. Signals on the top layer

The Board itself was easily assembled and all components were found to match footprints. The assemble board was found to be very rugged and is able to handle mechanical jolts that would be expected during humanoid operation. The board was found to effectively distribute heat from the components.

Chapter 8 Conclusion

As a result of work to date, the Power Supply will meet the power requirements of the humanoid. The design falls short of the 800W average power rating for 20 minutes, but can still provide 800W continuous, but with a reduced running time of around 10 minutes.

There has been a large fall in the simulated power requirements from those predicted at the start of the project when the design objective of 800W was set. Currently the average power required is 70W. With the design as is, this would extend the supplies lifetime to around 3hrs. Alternatively, the number of batteries could be reduced, to save weight. The control system envisaged for the board would be able to handle the hot swapping of any of the 42V packs. The extended operating time could equally be an attractive option, particularly during testing and refinement of control algorithms.

The Power Supply board has not been fully populated and needs to be completely tested. The Battery boards need to be manufactured, populated and installed on the batteries.

The control loops and algorithm are yet to be completely implemented but a first version should be finished by the end of the semester. Testing of the system, in regards to efficiency, stability and response to load changes, can be partially done once the board is constructed. The majority of testing can only be done once the completed GuRoo is functioning.

Once the GuRoo has been constructed, it would be beneficial to reassess the power requirements. This would give some idea as to how accurate the simulator is and could be used in the next revision of the power supply. Future work should include a redesign

of the board to reduce weight and size. Efforts to improve maximum power output, or the efficiency of the supply would be beneficial depending on the actual power requirements.

The Power Supply will power the GuRoo, even if it is very Power hungry.

Bibliography

1. Bebel, Bartek, *USB to CAN Bridge for Humanoid Project*, Undergraduate Thesis, University of Queensland 2001.
2. Burr Brown, INA122, *Single Supply MicroPower, Instrumentation Amplifier*, October 1997.
3. Blower, Andrew, *Development of a Vision System for a Humanoid Robot*, Undergraduate Thesis, University of Queensland, 2001.
4. C & D Technologies, *1400 SERIES Bobbin Type Inductors datasheet*, 2000.
5. Cartwright, Timothy, *Design and Implementation of Small Scale Joint Controllers for a Humanoid*, Undergraduate Thesis, University of Queensland 2001.
6. Dowling Ken, *Power Sources for Small Robots*, Field Robotics Centre, The Robotics Institute, Carnegie Mellon University, 1997.
7. Gold Peak, *Batteries - Nickel Metal Hydride (NiMH)*
<http://www.gpina.com/industrial/batteries/NiMH/NiMHspecs.htm>, accessed 10/10/2001
8. Herbert H. C. Iu, Chi K. Tse, *Instability and Bifurcation in Parallel-Connected Buck Converters Under a Master-Slave Current Sharing Scheme*, Annual Power Electronics Specialist Conference, 2000 pp 708-713.
9. Honda, *Humanoid Robot Specifications*, Honda Motor Co., Ltd.
<http://world.honda.com/robot/specifications/> , accessed 14/10/01

10. Honda, *The Humanoid Robot ASIMO, Specifications*. Honda Motor Co., Ltd.
<http://world.honda.com/ASIMO/spec/>, accessed 14/10/01
11. Hosking, Shane, *High Speed Peripheral Interface*, Undergraduate Thesis,
University of Queensland
12. Horowitz P., W. Hill, *The Art of Electronics, Second Ed.*, Cambridge University
Press, Cambridge, UK, 1989.
13. Intersil, *HIP2106 Data Sheet*, August 1999.
14. International Rectifier, *6CWQ03FN SCHOTTKY RECTIFIER 7 Amp PD-20560
rev. B datasheet*, October 1998.
15. International Rectifier, *IPS5451/IPS5451S Data Sheet No.PD60159-K FULLY
PROTECTED HIGH SIDE POWER MOSFET SWITCH*, August 2000.
16. International Rectifier, *IRF540N HEXFET Power MOSFET PD - 91341B
datasheet*, March 2001.
17. Letourneau Claude, David A. Wilmont, David C. Worboys, "*Lithium Polymer
Batteries – The Next Generation Power Source*", International
Telecommunications Energy Conference 1997, pp 87-91
18. Kee, Damien, *Design and Simulation of a Humanoid Drive System*,
Undergraduate Thesis, University of Queensland, 2001.
19. Lin J. L., Chen, S.J. 1996, *u-based Controller Design for a DC-DC Switching
Power Converter with Line and Load Variations*, IEEE IECON 96.
20. Lopez Mariano, J Luis Garcia de Vicuna, Miguel Castilla, Jose Matas, Oscar
Lopez, *Control Loop Design of Parallel Connected Converters Using Sliding*

Mode and Linear Control Techniques, Annual Power Electronics Specialists Conference, 2000, pp 390-394.

21. Mammano Robert, *Switching Power Supply Topology, Voltage Mode vs. Current Mode*, Electronic Design, Penton Publishing, 1994
22. Matsuo Hirofumi, Fujio Kurokawa, Haruhi Etou, Yoichi Ishizuka, Changfeng Chen, *Design Oriented Analysis of the Digitally Controlled DC-DC Converter*, Annual Power Electronics Specialists Conference, 2000, pp 401-407.
23. McMillain Scott, *Computational Dynamics for Robotic Systems on Land and Under Water*, PhD Dissertation, Ohio State University, 1995.
24. Mohan N., Underland T., Robbins W., 1989, *POWER ELECTRONICS: Converters, Applications, and Design*. John Wiley and Sons, New York
25. National Semiconductor, *LM1084 5A Low Dropout Positive Regulators*, August 2000.
26. National Semiconductor, *LM119/LM219/LM319 High Speed Dual Comparator*, August 2000.
27. National Semiconductor, *LM2586 SIMPLE SWITCHER datasheet*, May 1996
28. National Semiconductor, *LM35 Precision Centigrade Temperature Sensors*, November 2000
29. National Semiconductor, *LMC6081 Precision CMOS Single Operational Amplifier datasheet, 2000*
30. National Semiconductor, *LM611 Operational Amplifier and Adjustable Reference*, August 2000

31. Nise, N.S., *Control Systems Engineering, Third Edition*, John Wiley & Sons, New York, New York, 2000.
32. Panasonic, *Aluminium Electrolytic Capacitors/FC series datasheet*, 2000.
33. Panasonic, *Charge Methods for Ni-Cd Batteries*, Panasonic, 2000.
34. Panasonic, *Charge Methods for Nickel Metal Hydride Batteries*, January 2000.
35. Panasonic, *Choke Coils, types 06D, 09D, 10D, 16B, 18B, 10E, 12E, 15E, 18E, datasheet*, 2000.
36. Panasonic, *Nickel Cadmium Batteries: P-150AS Data Sheet*, Panasonic, 2000.
37. Panasonic, *Nickel Metal Hydride Batteries*, January 2000.
38. Panasonic, *Overview of Lithium Ion Batteries*, January 2000
39. Panasonic, *Precautions for designing devices with NiCd batteries*, January 2000.
40. Panasonic, *Rechargeable Nickel Cadmium Batteries*, Panasonic, 2000.
41. Phillips Semiconductor, *Rectifier Diodes, BYV32E, BYV32EB series*, July 1998
42. Phillips Semiconductor, *74HC/HCT541 Octal buffer/line driver; 3-state datasheet*, 1990
43. Prasser, David P., *Vision Software for Humanoid Robot Soccer*, Undergraduate Thesis, University of Queensland, 2001.
44. RoboCup, Robocup Web page, www.robocup.org, accessed 10/10/2001
45. Saft, *Medium Prismatic lithium-ion batteries*. Brochure, September 2000.

46. Saft, *Space Industry*, website, 2000, accessed 5/10/2001.
http://www.saftbatteries.com/space_industry/index.htm,
47. Smith, Andrew, *Simulator Development and Gait Pattern Creation for a Humanoid Robot*, Undergraduate Thesis, University of Queensland 2001.
48. Stirzaker Jarad Heath, *Design of DC Motor Controllers for a Humanoid Robot*, Undergraduate Thesis, University of Queensland, 2001.
49. Texas Instruments, *TMS320F243, TMS320F241 DSP Controllers*, Texas Instruments, Houston, Texas, 2000.
50. Wagstaff, Mark, *Mechanical design for a Humanoid*, Undergraduate Thesis, University of Queensland.
51. Wu Ren-Hau, Teruhiko Kohama, Yuichi Kodera, Tamotsu Ninomiya, Fumiaki Ihara, *Load-Current Sharing Control for Parallel Operation of DC-to-DC Converters*, Annual Power Electronics Specialists Conference, 1993, pp 101-107.
52. Wyeth, G, 2001, *Design of an Autonomous Humanoid Robot*, University of Queensland, Brisbane
53. Zelniker, Emanuel, *Joint Control for an Autonomous Humanoid Robot*, Undergraduate Thesis, University of Queensland, 2001.

Appendix

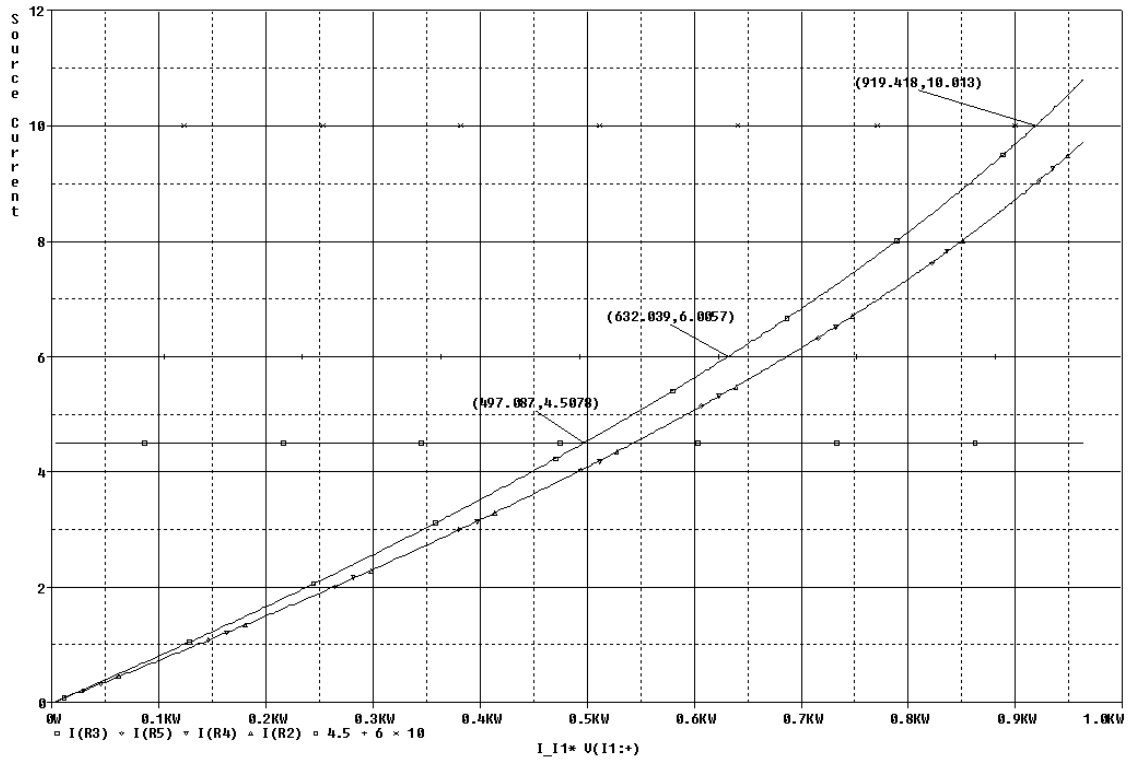


Figure 0-1 Power Output vs. Source Current Batteries with diodes in series, all sources at 35V, 3 at 1Ω, 1 at 0.9Ω.

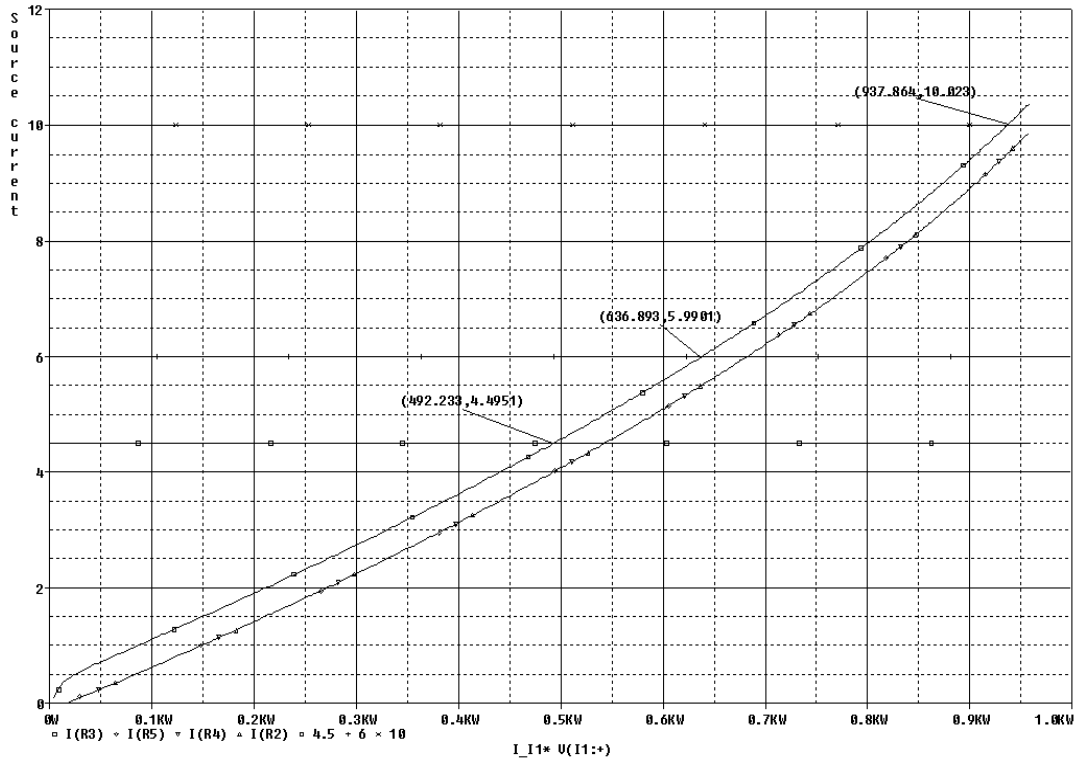


Figure 0-2 Power out (kW) vs. Source Current (A). All sources at 1Ω, 3 at 35V one at 35.5V

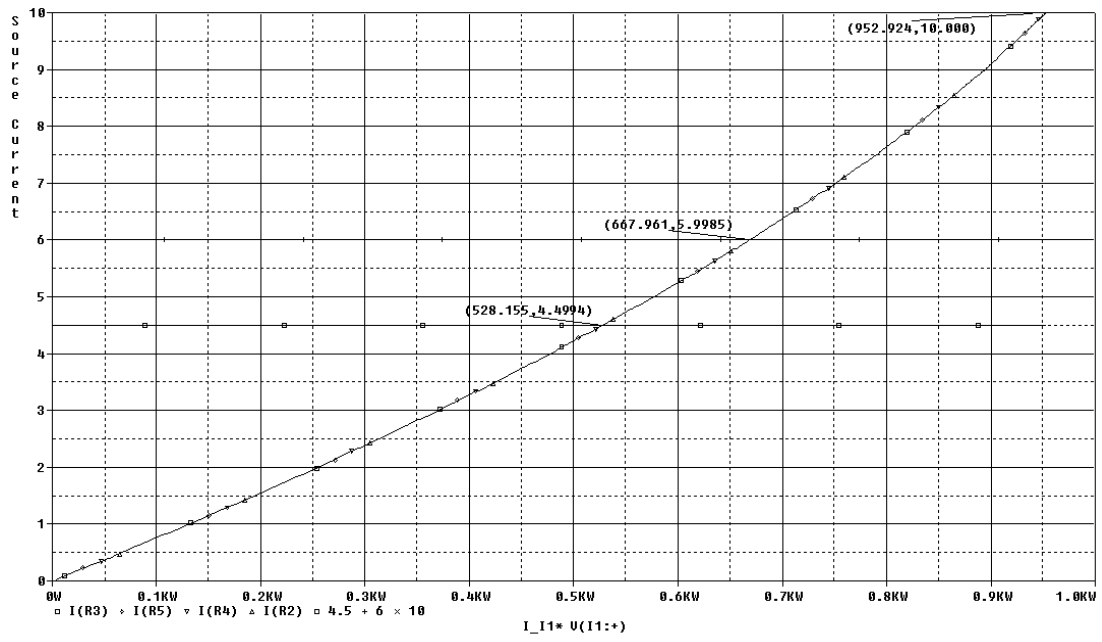


Figure 0-3 Power out (kW) vs Source Current (A), ideal case all at 35V 1Ω.

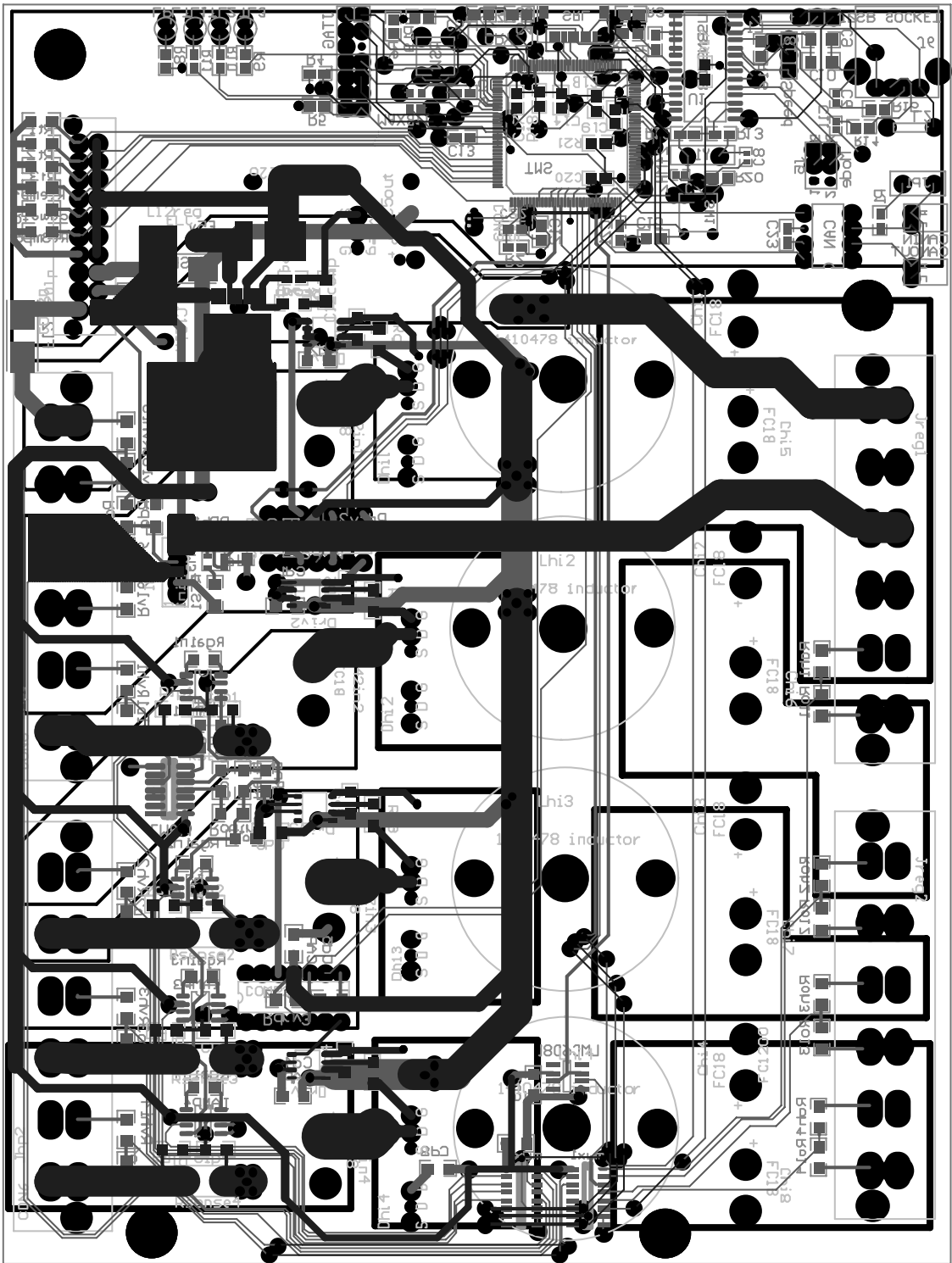


Figure 0-4 Power Board PCB